

UNCLASSIFIED



AD NUMBER

AD-921 078

NEW LIMITATION CHANGE

TO

DISTRIBUTION STATEMENT - A

Approved for Public Release; Distribution Unlimited.

Limitation Code: 1

FROM

DISTRIBUTION STATEMENT - B

U.S. Gov't Agencies Only.

Limitation Code: 3

AUTHORITY

AFATL, via ltr., dtd April 5, 1976.

THIS PAGE IS UNCLASSIFIED

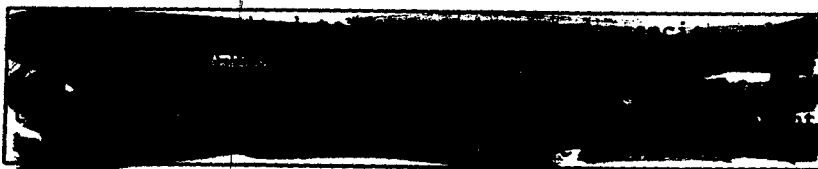
AFATL-TR-74-86

**COMPILATION OF SURFACE TARGET  
VULNERABILITY AND EFFECTIVENESS  
METHODOLOGIES**

BOOZ, ALLEN AND HAMILTON, INC.  
P.O. BOX 874  
SHALIMAR, FLORIDA 32579

MAY 1974

FINAL REPORT FOR PERIOD 5 DECEMBER 1972-31  
JANUARY 1974



**AIR FORCE ARMAMENT LABORATORY**

AIR FORCE SYSTEMS COMMAND • UNITED STATES AIR FORCE

EGLIN AIR FORCE BASE, FLORIDA

Reproduced From  
Best Available Copy

19991012153

AD921078

UNCLASSIFIED

SECURITY CLASSIFICATION OF THIS PAGE (When Data Entered)

REPORT DOCUMENTATION PAGE		READ INSTRUCTIONS BEFORE COMPLETING FORM
1. REPORT NUMBER AFATL-TR-74-86	2. GOVT ACCESSION NO.	3. RECIPIENT'S CATALOG NUMBER
4. TITLE (and Subtitle) COMPILATION OF SURFACE TARGET VULNERABILITY AND EFFECTIVENESS METHODOLOGIES		5. TYPE OF REPORT & PERIOD COVERED Final Report - 5 December 1972 to 31 January 1974
		6. PERFORMING ORG. REPORT NUMBER
7. AUTHOR(s) William R. Day Phillip A. Kimble		8. CONTRACT OR GRANT NUMBER(s) F08635-72-C-0082
9. PERFORMING ORGANIZATION NAME AND ADDRESS Booz, Allen & Hamilton, Inc. P.O. Box 874 Shalimar, Florida 32579		10. PROGRAM ELEMENT PROJECT, TASK AREA & WORK UNIT NUMBERS Project No. 9134 Task No. 06 Work Unit No. 001
11. CONTROLLING OFFICE NAME AND ADDRESS Air Force Armament Laboratory Air Force Systems Command Eglin Air Force Base, Florida 32542		12. REPORT DATE May 1974
14. MONITORING AGENCY NAME & ADDRESS (if different from Controlling Office)		13. NUMBER OF PAGES 78
		15. SECURITY CLASS. (of this report) UNCLASSIFIED
		15a. DECLASSIFICATION DOWNGRADING SCHEDULE
16. DISTRIBUTION STATEMENT (of this Report): Distribution limited to U.S. Government Agencies only; this report documents test and evaluation; distribution limitation applied May 1974. Other requests for this document must be referred to the Air Force Armament Laboratory (DLRV), Eglin Air Force Base, Florida 32542.		
17. DISTRIBUTION STATEMENT (of the abstract entered in Block 20, if different from Report)		
18. SUPPLEMENTARY NOTES Available in DDC		
19. KEY WORDS (Continue on reverse side, if necessary, and identify by block number) Surface Target Vulnerability      Parametric Weapon System Lethality Weapons Effectiveness Analysis      Analyses Damage Criteria Kill Probability Estimates		
20. ABSTRACT (Continue on reverse side, if necessary, and identify by block number) The Surface Target Subgroup of the Joint Technical Coordinating Group/Munitions Effectiveness (JTCCG/ME) is sponsoring an effort for compilation of target test data and vulnerability methodologies. As part of that effort, this report has been prepared to provide a ready reference to analytical and empirical relationships which are used in target vulnerability and weapon system effectiveness computer simulation routines. The principal intent of this compilation is to provide the target vulnerability analyst with an overview		

DD FORM 1 JAN 73 1473 EDITION OF 1 NOV 65 IS OBSOLETE

UNCLASSIFIED

SECURITY CLASSIFICATION OF THIS PAGE (When Data Entered)

UNCLASSIFIED

SECURITY CLASSIFICATION OF THIS PAGE(When Data Entered)

of the various methodologies used in weapons effectiveness analysis routines which relate target physical and vulnerability descriptions to damage criteria, kill probability estimates, and parametric weapon system lethality analyses. This document should promote a better understanding of how target vulnerability data is currently used, and how future target vulnerability definitions may be structured to take advantage of improvements in available data and computer technology. The format and level of detail in this report presupposes the availability to the reader of the Basic Joint Munitions Effectiveness Manual for Air to Surface, Weapon Effectiveness Selection and Requirements (Reference 1) and some familiarity with its contents.

UNCLASSIFIED

SECURITY CLASSIFICATION OF THIS PAGE(When Data Entered)

## SUMMARY


The Surface Target Subgroup of the Joint Technical Coordinating Group/Munitions Effectiveness (JTCC/ME) is sponsoring an effort for compilation of target test data and vulnerability methodologies. As part of that effort, this report has been prepared to provide a ready reference to analytical and empirical relationships which are used in target vulnerability and weapon system effectiveness computer simulation routines. The principal intent of this compilation is to provide the target vulnerability analyst with an overview of the various methodologies used in weapons effectiveness analysis routines which relate target physical and vulnerability descriptions to damage criteria, kill probability estimates, and parametric weapon system lethality analyses. This document should promote a better understanding of how target vulnerability data is currently used, and how future target vulnerability definitions may be structured to take advantage of improvements in available data and computer technology. The format and level of detail in this report presupposes the availability to the reader of the Basic Joint Munitions Effectiveness Manual for Air to Surface, Weapon Effectiveness Selection and Requirements (Reference 1) and some familiarity with its contents.

## PREFACE

This report partially documents work accomplished during the period 5 December 1972 through 31 January 1974 by Booz, Allen & Hamilton, Inc., P.O. Box 874, Shalimar, Florida, under Contract No. F08635-72-C-0082 with the Air Force Armament Laboratory, Eglin Air Force Base, Florida. The program monitors for the Armament Laboratory were Mr. G. Rickey Griner and Mr. J. Michael Heard (DLRV).

The report documents that effort of the above contract directed toward compilation of surface target vulnerability and munition effectiveness methodologies available to the vulnerability community. It contains a reference list of 61 documents which are typified in this report by the analytical and empirical relationships presented therein.

This technical report has been reviewed and is approved for publication.

  
CHARLES K. ARPKE, Lt Colonel, USAF  
Chief, Weapons Effects Division

## TABLE OF CONTENTS

Section	Page
I. INTRODUCTION . . . . .	7
II. PHYSICAL DESCRIPTION MODELS AND DIRECT HIT METHODOLOGY . . . . .	10
Direct Hit Effectiveness Indices . . . . .	10
Direct Hit Physical Simulation Models . . . . .	11
Point Location, Circular and Rectangular Models . . . . .	11
Parallelepiped, Spherical, and Cylindrical Models For Direct Hit . . . . .	13
Quadric Surface Models . . . . .	17
Planar Surface Fitting Models . . . . .	26
III. BLAST DAMAGE VULNERABILITY SIMULATION MODELS . . . . .	30
Blast Damage Effectiveness Indices . . . . .	30
Blast Physical Simulation Models . . . . .	31
Two-Dimensional Models . . . . .	31
Three-Dimensional Models . . . . .	34
Blast Damage as a Function of Distance . . . .	36
Atmosphere and Other Variable Dependent Models . . . . .	37
IV. FRAGMENTATION DAMAGE EFFECTIVENESS METHODOLOGY . . . . .	39

## TABLE OF CONTENTS (CONCLUDED)

Section	Page
Fragmentation Damage Effectiveness Indices . . . . .	39
Fragment Physical Simulation Models . . . . .	44
Fragmenting Munition Effectiveness Analysis . . . . .	44
Multiple Fragment and Synergistic Effects . . . . .	49
V. MISCELLANEOUS SPECIAL PURPOSE VULNER- ABILITY METHODOLOGY. . . . .	50
Incendiary/Fragmentation Munition Models . . . . .	50
Burning Particle Projection . . . . .	51
Fuel Container Perforation . . . . .	52
Fuel Cavitation and Spray Emergence . . . . .	53
Fuel Cavitation and Spray Pulses . . . . .	54
Shaped Charge Munition Models. . . . .	56
Flechette Projecting Munition Models . . . . .	62
Warhead Methodology . . . . .	65
Trajectory Analysis . . . . .	65
Lethal Area Computations . . . . .	67
REFERENCES . . . . .	70



## LIST OF ILLUSTRATIONS

Figure	Title	Page
1.	Direct Hit of Target Complex Elements . . . . .	14
2.	Quadric Surface Models . . . . .	18
3.	Penetration of an Ellipsoid . . . . .	19
4.	End View of Penetrated Ellipsoid . . . . .	22
5.	Top View of Penetrated Ellipsoid . . . . .	22
6.	Impact Angle to Target Surface . . . . .	24
7.	SHOTGEN Model . . . . .	27
8.	TARGET DESCRIPTION Model . . . . .	28
9.	COMGEOM Model . . . . .	29
10.	Effective Miss Distance About a Rectangular Target . . .	33
11.	Effective Target Area . . . . .	33
12.	Blast Ellipsoid Around Box-Shaped Target . . . . .	35
13.	Probability of Blast Kill Versus Distance . . . . .	36
14.	SHOTLINE Grid . . . . .	43
15.	Shaped Charge Geometry . . . . .	56
16.	Fragment Spray Representation . . . . .	60
17.	Sample Warhead Geometry . . . . .	63
18.	Trajectory Geometry . . . . .	66
19.	Sample Impact Pattern Geometry . . . . .	67

## SECTION I

### INTRODUCTION

This report presents a survey of surface target weapon system effectiveness computer programs performed for the Target Vulnerability Panel of the Joint Technical Coordinating Group on Munitions Effectiveness (JTCG/ME). The purpose of the survey was to identify necessary input data to the effectiveness programs relating to the target systems, so that present and future target vulnerability assessments meet those input requirements. The survey showed the existence of numerous simulation models, with new models being developed. Most weapon system effectiveness models are ad hoc efforts written and used to counter a critical emergency or to exploit a crucial opportunity, and then filed away to be recalled and modified as required. Most are never documented at all; many are documented too poorly to be used by anyone but the original developer; some, not many, are fully documented.

Identifying the latter category of well-documented, frequently-used, and widely-accepted computer programs for inclusion in the methodology survey of this report was a desirable but elusive goal. Many worthy programs may have been ignored, preemptorily discarded, or not discovered. Many more may have been included in the survey which should have been discarded since they offered nothing unique, but were modified versions of similar programs or inferior, stripped-down replicas of more sophisticated models.

Of those programs examined, there were basically two levels of sophistication:

- Models containing efficient closed-form or open-end curve fitting mathematical expressions, and
- Models containing iterative integral solutions such as Monte Carlo random sampling techniques, Gaussian, Hermitian, or LeGendre integration.

Examples of particular types of programs by name, and recommendations for sources of methodology will be made, but no attempt will be made to catalog all the methodology sources for each type of program since such

was not the purpose of this survey. A brief description of the methodology available for use by the weapon system analyst and some remarks about the degree of appropriateness of such use has been the objective.

For air-to-surface target vulnerability and weapon effectiveness evaluation, the JTCG/ME has established standards for computer programs and has published documentation for acceptable air-to-surface computer methodology as a part of the Joint Munitions Effectiveness Manuals, Air-to-Surface (Reference 2). The methodology includes simplified open-end methods, documented in and developed for use with the Basic Manual (Reference 1), as well as more sophisticated methodology published in a separate methodology volume (Reference 3). In addition, a number of well defined special purpose computer programs are published as separate documents by JTCG/ME (for a listing of these programs and a short description of their application, see Reference 4). These methodologies are in the process of revision, updating, and improvement and are not intended to be the final work in air-to-surface methodology. The methodologies have been widely used, however, and have proved to be of reasonable accuracy for most of the demands and applications of weapon systems analysts.

These JMEM-accepted methodologies are available for use (often with many minor modifications) within the weapons effectiveness analysis community. They will not fulfill every need of the weapons analyst, but they do provide much of the basic framework for developing new computer programs for use with unique products of research and development and may be considered entirely adequate for establishing weapons lethality and force requirements for most inventory munitions. In every case where a need for effectiveness analysis is established, these approved methodologies should be considered for use in their pure or modified forms and all new superior methodology which must be developed should be submitted to the appropriate committees for review and possible inclusion within the list of acceptable JMEM methodologies.

The following sections contain discussions of various methodologies for computing target vulnerability and weapon effectiveness. The measure of effectiveness or desired outcome of all such computations is single shot probability of damage ( $SSP_D$ ) or, as it is sometimes called, single shot kill probability ( $P_{KSS}$ ), which in three-dimensional Cartesian coordinates is given by:

$$P_{KSS} = \iiint P_{KT}(x, y, z) F(x, y, z) dx dy dz \quad (1)$$

where  $P_{KT}$  is the total kill probability for all kill mechanisms from a munition detonating at point  $(x, y, z)$ , and  $F(x, y, z)$  is a distribution density function defining the likelihood of the munition detonating within the infinitesimal intervals  $dx$ ,  $dy$ , and  $dz$  about each point  $(x, y, z)$ . The total kill is a composite of kills from all applicable mechanisms of a given warhead combined in the following manner:

$$P_{KT} = 1 - (1 - P_{KDH})(1 - P_{KB})(1 - P_{KF})(1 - P_{KI}) \dots \quad (2)$$

where  $P_{KDH}$  is the kill probability from direct hit effects,  $P_{KB}$  is the kill probability from blast effects,  $P_{KF}$  is the kill probability from fragmentation effects, and  $P_{KI}$  is the kill probability from incendiary effects, continuous rod, shaped charge jets, etc. The individual kill probabilities are normally obtained using computerized simulation models which are the subject of the succeeding sections.

The distribution density functions  $F(x, y, z)$  in Equation (1) are the statistical formulae for measure of dispersion: mean, variance, and standard deviation. Most of the programs use a random normal or Gaussian distribution for determining individual weapon system ballistic dispersion, and since the variance is normally fixed for the  $Z$  (altitude) dimension and independent for the other two dimensions ( $X$  and  $Y$ ), a bivariate normal distribution is almost universally used for surface target effectiveness evaluation programs. For cluster munitions and stick releases the distribution may be random uniform within the pattern intervals or uniformly spaced for intervalometer releases. Only one of the programs reviewed used a modified Rayleigh Distribution for ballistic dispersion, and no other type of dispersion was discovered.

## SECTION II

### PHYSICAL DESCRIPTION MODELS AND DIRECT HIT METHODOLOGY

Perhaps the most readily apparent distinction between the highly efficient simple programs and the more sophisticated and time-consuming integral models is the degree of accuracy with which a target element or complex can be mathematically simulated for evaluation with the several damage mechanisms. As a general rule for the programs examined, the most sophisticated target models were contained in the more complicated programs. Older programs were much less concerned with realistic direct hit target models since the direct hit kill mechanism has only recently (with the advent of electro-optical, laser, and infrared terminally guided weapons) become a major consideration. A realistic physical model in an endgame effectiveness analysis program is only considered important to accurately predict damage from a direct hit or very near miss of a target element by an individual munition.

### DIRECT HIT EFFECTIVENESS INDICES

Existing vulnerability data for the direct hit kill mechanism are quite simple in form. Only three types of direct hit effectiveness indices (EI) are currently defined: the vulnerable area (VA), probability of damage given a hit ( $P_{HD}$ ), and bridge effectiveness index (BEI). The VA of a target is that area which is vulnerable to the damage mechanisms of a given weapon. In computing weapon requirements, it is used as a measure of the effectiveness for a weapon/target combination requiring a direct hit. VA usually is not associated with any particular segment of the target but is a measure of the vulnerability of the target as a whole. However, the term "vulnerable area" can sometimes be applied to a particular segment of a target when conditions are such that only a particular segment of the total target is vulnerable to that weapon. In that case, the probability of damage given a hit ( $P_{HD}$ ) is unity over the segment defined as the vulnerable area (an example is a dam target whose VA would be the floodgate or spillway).

The number associated with VA is mathematically arrived at by dividing the total area within which the weapon can affect the target into small units, each with area  $A_i$ . Then, the probability of damage given a hit on that area ( $P_{HDI}$ ) is found for each unit area, and the sum of the products ( $P_{HDI})(A_i)$  is defined as the VA of the target.

The VA is applied to the calculation of the probability of damage given a random direct hit on the target ( $P_{HD}$ ). The  $P_{HD}$  is equal to the ratio of the VA to the total presented area of the target.

For a given munition the  $P_{HD}$  may be a single value which, due to lack of data, is usually assumed by the analyst to be either zero or one. For those targets for which data exist, a table of  $P_{HD}$  values may be specified as a function of weapon delivery parameters such as terminal velocity or elevation angle.

The third form of EI for direct hit kill, the BEI, is used currently for specialized bridge targets only. The BEI expresses the conditional damage probability ( $P_{HD}$ ) as a function of the bridge width ( $W_b$ ) using the equation:

$$P_{HD} = 1 - e^{-\frac{BEI}{W_b}} \quad (3)$$

The BEI is an empirically derived constant which has been developed to describe the effectiveness of a particular weapon against a particular bridge type.  $P_{HD}$  in this usage represents the statistical probability of causing a sufficient level of damage from a random direct hit on the bridge roadbed. Similar data for roads, railroads, and aircraft taxiways or runways could possibly fill a void which exists in the analysts arsenal of effectiveness methodology.

## DIRECT HIT PHYSICAL SIMULATION MODELS

### Point Location, Circular and Rectangular Models

There is currently a class of effectiveness models, used not infrequently, which totally ignores the possibility of a direct hit on the target. In this type of program, the target element or elements are defined only by a two- or three-dimensional coordinate point location (i.e., the target may be located at (X, Y) or (X, Y, Z), but no size, shape, or description is specified for direct hit computations). Examples of this type of program are given in References 5 through 13.

Only slightly more sophisticated is a two-dimensional model in very wide use within many effectiveness analysis programs. This representation of the target is often used for single target elements, multielement complexes, or for both elements and complexes within the same program. Most of the routines which use a two-dimensional physical description model use either a circle or a rectangle in or parallel to the ground plane to represent the target; some permit a choice, and a few even extend the choice to include an ellipse.

When a circular, rectangular, or elliptical area is used to represent a single target element, the radius, (X, Y) dimensions, or major and minor axes are normally specified so that the interior of the planar figure encloses an area equal to the average presented area of the target from the weapon attack aspects. Almost universally, though, the practice is to use an estimate of the presented area from the 90-degree elevation (overhead) aspect without regard to weapon delivery parameters. This simplification is necessary partly because tabulated presented areas from various aspects are not readily available for most target types. However, even with exceptional targets for which these data are available, the increased accuracy to be achieved in a two-dimensional model hardly warrants the effort to include this added precision. References 14 through 21 are some of the best examples of programs using two-dimensional models for unitary targets or complex target areas.

To represent a complex target composed of many identical elements, it is normally assumed that the elements are distributed in a uniformly random manner over the entire surface area of the target complex (circle ellipse, or rectangle). For this type of simulation, most computer models totally ignore direct hit kill of elements. This omission is not serious if the area of a target element times the number of elements is small compared to the complex area. Even if this is not the case and the ignored direct hit kill probability would be large, the error is usually compensated for (sometimes overcompensated) by the statistical methods for estimating blast or fragmentation kill (see succeeding sections).

The major attractions of two-dimensional physical models to the effectiveness analyst are simplicity, speed, and minimal usage of computer time. For simple targets such as a runway, railroad yard, warehouse, highway, or bridge roadbed, the model is sufficiently accurate. Also, there are occasions when precision is of minor importance (e.g., when computing gross trends from large amounts of parametric data). The simplicity of the two-dimensional model permits very comprehensive simulations to be made in a single computer run.

For example, the attack of a target complex consisting of hundreds of individually defined circular or rectangular targets by a B-52 formation dispersing tens of thousands of submunitions may be simulated with such simple models whereas use of a more complicated model would be impracticable. The best results for two-dimensional physical models are obtained when estimating direct hit probabilities for high altitude bombing tactics with large numbers of bomblet munitions or multiple passes against a single or multiple element complex. The poorest results are obtained when simulating low level bombing tactics, artillery delivered munitions, and terminally guided weapons.

The mathematical formulations for two-dimensional direct hit models are obvious for a single target and single munition. For a multielement complex target and a uniform distribution of munitions, the statistical formula of Equation (4) for  $F_K$  (fractional kill) is an example of the best methodology used in a closed-form program.

$$F_K = 1 - \left( 1 - P_{HD} \frac{nA_E}{\pi R_C^2} \right)^m \quad (4)$$

where  $P_{HD}$  is the probability of kill given a direct hit on a single target element,  $n$  is the number of target elements in the complex,  $A_E$  is the presented area of a single target element,  $R_C$  is the radius of the circular target complex, and  $m$  is the total number of munitions falling within the area defining the target complex.

#### Parallelepiped, Spherical, and Cylindrical Models for Direct Hit

The next level of accuracy for surface target effectiveness program physical description models employs parallelepipeds or, occasionally, spheres and cylinders to simulate the actual configuration of a target element. This methodology is almost universal among the high-accuracy programs using Gaussian or Monte Carlo integral solutions, and although the descriptive accuracy is very poor compared to target vulnerability assessment models or air target physical simulation models, it has, in the past, been considered by most effectiveness analysts to be wholly adequate for surface target weapons lethality assessment of direct hit kill capability. Nearly all of the large-scale effectiveness programs



reviewed which contained a three-dimensional target model use a single parallelepiped to model a target element. Each target element is described by a point location (vulnerable area centroid), a length, width, and height. The most sophisticated large-scale models also define an element orientation angle to permit rotation of the target element in the ground plane, and permit definition of non-target elements such as revetments or nearby structures which would protect or shield the target element from a direct hit or fragmentation kill.

Figure 1 illustrates a typical description of a complex consisting of two vulnerable elements and a revetment. Three warhead trajectories are shown, one intersecting a surface of each component. The mathematical formulation to determine if an intersection occurs is given below.

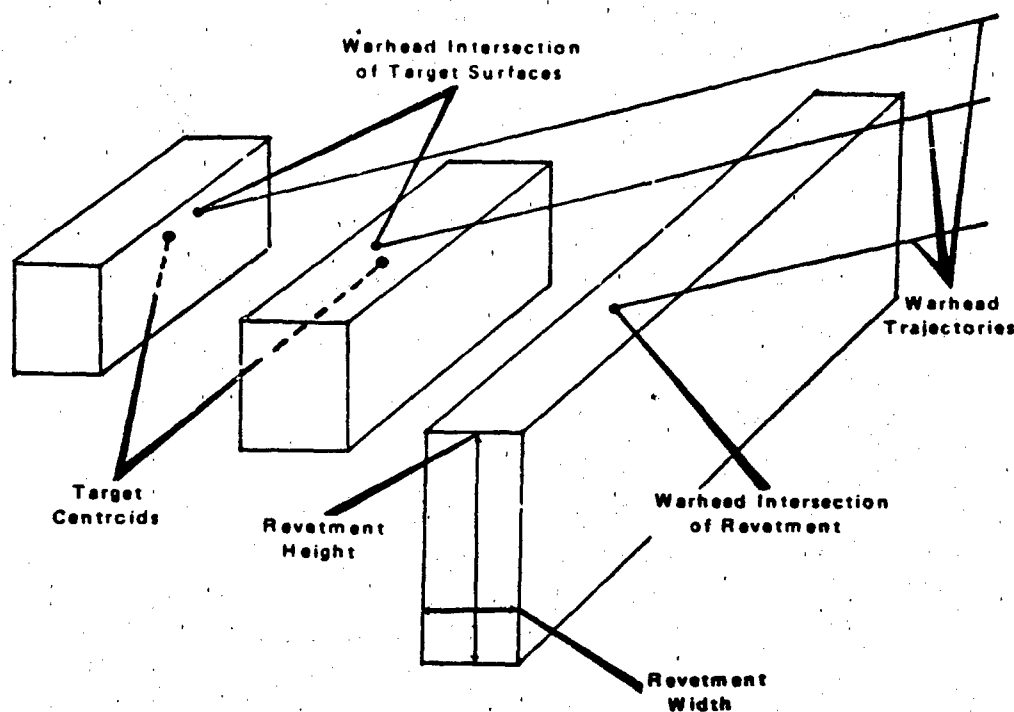


Figure 1. Direct Hit of Target Complex Elements

If the defining physical surfaces of a target complex are represented as a series of horizontal and vertical rectangles, a direct hit will occur if a line defining the warhead trajectory intersects any one of the planar surfaces of a target element prior to detonation. This trajectory line can be represented by two points  $(X_W, Y_W, Z_W)$  and  $(X_T, Y_T, Z_T)$ . The equation of the line is given by:

$$\frac{X - X_T}{X_W - X_T} = \frac{Y - Y_T}{Y_W - Y_T} = \frac{Z - Z_T}{Z_W - Z_T} \quad (5)$$

The horizontal or vertical rectangular element can also be represented by two sets of coordinates. For example, the first point  $(X_1, Y_1, Z_1)$  is located at the bottom end of a vertical surface, and the second point  $(X_2, Y_2, Z_2)$  is located at the top of the other end (diagonal) of the surface. Using these two points and a third  $(X_f, Y_f, Z_f)$  derived from them, a plane representing the surface can be formulated in matrix notation as follows:

$$\begin{bmatrix} X & Y & Z & 1 \\ X_1 & Y_1 & Z_1 & 1 \\ X_2 & Y_2 & Z_2 & 1 \\ X_f & Y_f & Z_f & 1 \end{bmatrix} = 0 \quad (6)$$

Equation (6) defines the vertical plane containing the three points, and can be reduced to the following relation:

$$X(Y_1 Z_1 + Y_2 Z_2 - Y_1 Z_2 - Y_2 Z_1) - Y(X_1 Z_1 + X_2 Z_2 - X_1 Z_2 - X_2 Z_1) - (X_1 Y_2 Z_2 + Z_1 X_2 Y_1 - X_1 Y_2 Z_1 - Z_2 X_2 Y_1) = 0 \quad (7)$$

For simplicity, the following substitutions are employed:

$$A = Y_1 Z_1 + Y_2 Z_2 - Y_1 Z_2 - Y_2 Z_1 \quad (8)$$

$$B = X_1 Z_1 + X_2 Z_2 - X_1 Z_2 - X_2 Z_1 \quad (9)$$

$$D = X_1 Y_2 Z_2 + Z_1 X_2 Y_1 - X_1 Y_2 Z_1 - Z_2 X_2 Y_1 \quad (10)$$

Thus, the equation of the plane is given by:

$$AX - BY - D = 0 \quad (11)$$

Solving the equation of the line, Equation (5) for X and Y in terms of Z yields:

$$X = \frac{(Z - Z_T)(X_W - X_T)}{Z_W - Z_T} + X_T \quad (12)$$

$$Y = \frac{(Z - Z_T)(Y_W - Y_T)}{Z_W - Z_T} + Y_T \quad (13)$$

Substituting Equations (12) and (13) into Equation (11) gives the following relation:

$$Z = \frac{A [(Z_T)(X_W - X_T)(Z_W) + B(Y_T)(Z_W - Z_T)(Y_W) + D(Z_W - Z_T)]}{A(X_W - X_T) - B(Y_W - Y_T)} \quad (14)$$

The value of Z obtained from Equation (14) substituted into Equations (12) and (13) gives the X and Y coordinates of the intersection of the plane and the line.

The components for the point of intersection are checked to determine if they are actually contained within the bounds of the rectangular surface (e.g., is  $Z_1 < Z < Z_2$ ). Each check is performed by a series of comparisons for each coordinate value.

There are also available a few surface target effectiveness analysis programs which more realistically model target elements using a number of parallelepipeds for a single target element model. Although these programs are currently in use, they are recent developments for evaluating terminally guided bombs, and, as such, are almost completely undocumented. Since most are simply modifications of existing programs, it is unlikely that complete documentation will ever be available. The methodology for direct hit determination is identical to that for a single box description except that more surfaces must be checked. A typical example of a highly sophisticated three-dimensional direct hit evaluation model is contained in the Air Force Armament Laboratory's Program 1721 (see References 22, 23, and 24).

#### Quadric Surface Models

Although, among the programs which were reviewed, there were no surface target endgame effectiveness analysis routines which use quadric surface direct hit models to simulate a target physical configuration, it is nevertheless appropriate to include a brief description of this methodology. A surface which can be defined by a second degree equation is called a quadric surface. The formulations are available (References 25 and 26) and provide much greater accuracy than current models although they consume more core space and computer time. There is currently much sentiment for and some effort directed toward using quadric surfaces in a new family of high accuracy endgame effectiveness analysis programs for surface targets. Quadric surfaces have long been used for both air target effectiveness evaluation programs and for target vulnerability assessment where target physical descriptions are of paramount importance to accurate lethality evaluation.

In Lagrangian coordinates, each point (X, Y, Z) on a quadric surface will be a solution to an equation of the form:

$$AX^2 + BY^2 + CZ^2 + DXY + EXZ + FYZ + GX + HY + PZ + Q = 0 \quad (15)$$

Surfaces produced by straightline generators (cylinders and cones) and curves of revolution (spheres, ellipsoids, paraboloids, and hyperboloids) are special cases of such quadric surfaces. Other quadric surfaces include regular ellipsoids, hyperboloids, and paraboloids, and combined forms such as elliptic cylinders, elliptic cones, elliptic paraboloids, and hyperbolic paraboloids.

All of the above named surfaces have relatively simple closed-form defining equations and can be used alone or in combination to define or approximate many very complex shapes or figures. For example, Figure 2 illustrates how a MIG-21 can be quite adequately represented by six ellipsoids.

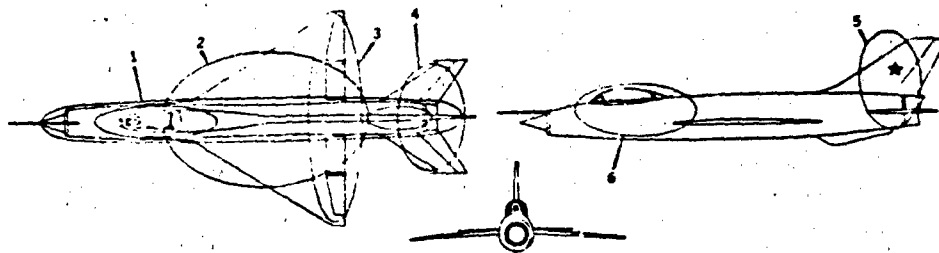


Figure 2. Quadric Surface Models

Since both the quadric surface and the weapon trajectory line can be precisely defined in a closed-form mathematical equation, a simultaneous solution of the two equations will define any and all points of intersection to accurately predict direct hit of the simulated target component or element. An example of the methodology for determining the intersection of a line and an ellipsoid follows (from Reference 25).

Consider an ellipsoid with axes of length  $2\alpha$ ,  $2\beta$ , and  $2\gamma$  located with the center at the origin of coordinate system B with coordinate axes  $X_B$ ,  $Y_B$ , and  $Z_B$ . As shown in Figure 3, the weapon trajectory line penetrates the ellipsoid at points  $P_1$  and  $P_2$ , which are along the X axis of the weapon (P) coordinate system and crosses the  $X_B$ ,  $Y_B$  plane at point A. A vector from the origin to point A is designated:

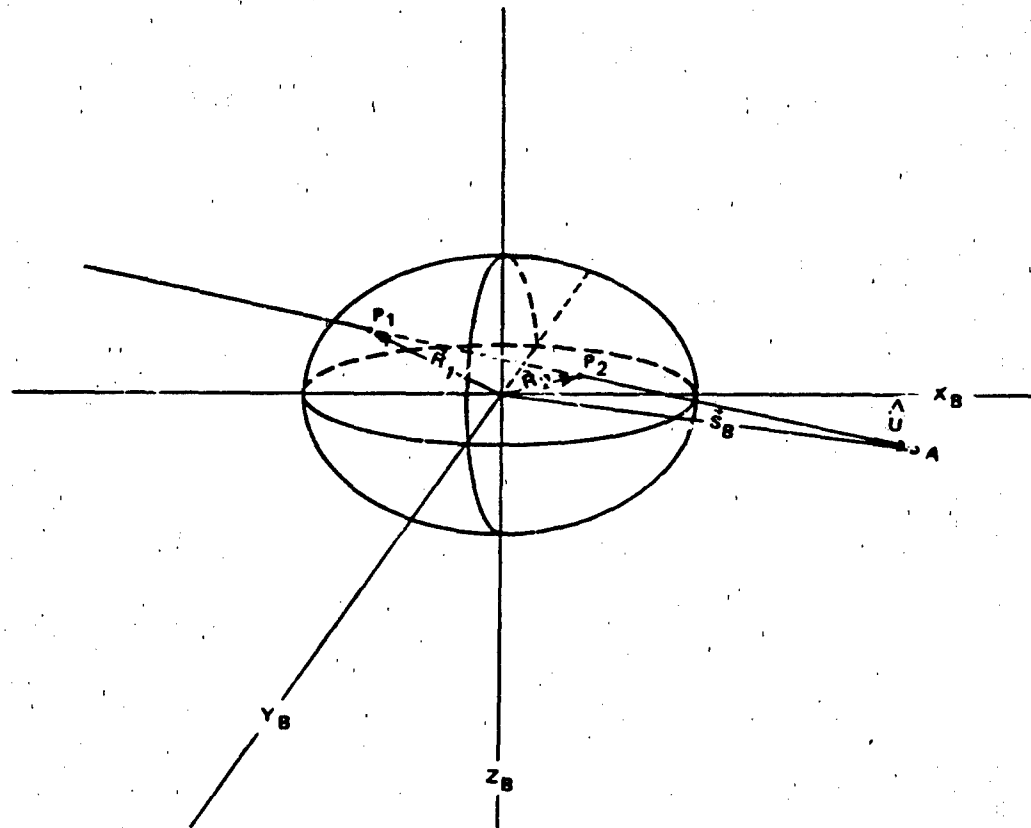


Figure 3. Penetration of an Ellipsoid

$$\vec{S}_B = x_B \hat{i}_B + y_B \hat{j}_B \quad (16)$$

A unit vector  $\hat{U}$ , measured in the P system, can be placed along the weapon path. Since the weapon is moving parallel to the  $X_P$  axis, the analytic representation of this unit vector will be:

$$\hat{U}_P = 1 \hat{i}_P + 0 \hat{j}_P + 0 \hat{k}_P \quad (17)$$

Vector  $\hat{U}_P$ , may be represented in the body coordinate system as  $\hat{U}_B$  by application of the rotation matrix T or:

$$\hat{U}_B = \hat{U}_P T \quad (18)$$

$$\hat{U}_B = [1, 0, 0] \begin{bmatrix} \cos \theta \cos \psi & -\cos \theta \sin \psi & \sin \theta \\ \sin \psi & \cos \psi & 0 \\ -\sin \theta \cos \psi & \sin \theta \sin \psi & \cos \theta \end{bmatrix} \quad (19)$$

where  $\theta$  and  $\psi$  are the elevation and azimuth of the weapon in the body coordinate system. Expressing  $\hat{U}_B$  in vector form:

$$\hat{U}_B = \cos \theta \cos \psi \hat{i} - \cos \theta \sin \psi \hat{j} + \sin \theta \hat{k} \quad (20)$$

For ease of notation, denote the coefficients of  $\hat{i}$ ,  $\hat{j}$ ,  $\hat{k}$  in the B system by  $x_u$ ,  $y_u$ , and  $z_u$ , hence:

$$x_u = \cos \theta \cos \psi \quad (21)$$

$$y_u = -\cos \theta \sin \psi \quad (22)$$

$$z_u = \sin \theta \quad (23)$$

From Figures 4 and 5 it can be seen that the coordinates of the points  $P_1$  and  $P_2$  are:

$$x_i = x_B - a_i x_u \quad (24)$$

$$y_i = y_B - a_i y_u \quad (25)$$

$$z_i = -a_i z_u \quad (26)$$

where  $i$  is either 1 or 2 and  $a_i$  denotes a scalar quantity, either  $a_1$  or  $a_2$ .

The general equation of an ellipsoid with reference to the body coordinate system is:

$$\frac{x^2}{\alpha^2} + \frac{y^2}{\beta^2} + \frac{z^2}{\gamma^2} = 1 \quad (27)$$

where  $\alpha$ ,  $\beta$ , and  $\gamma$ , are semiaxes of the ellipsoid. Then, substituting the values of  $x$ ,  $y$ , and  $z$  from Equations (24) through (26) for the points  $P_1$  and  $P_2$  gives:

$$(\beta\gamma)^2 (x_B - a_i x_u)^2 + (\alpha\gamma)^2 (y_B - a_i y_u)^2 + (\alpha\beta)^2 (-a_i z_u)^2 = (\alpha\beta\gamma)^2 \quad (28)$$

From Equations (21) through (23) and Equation (28), the values of the unknown scalar quantity  $a_i$  can be determined by solving the quadratic in  $a_i$  and substituting the values of  $x_u$ ,  $y_u$ , and  $z_u$ .

$$a_i = \frac{-B \pm \sqrt{B^2 - 4AC}}{2A} \quad (29)$$



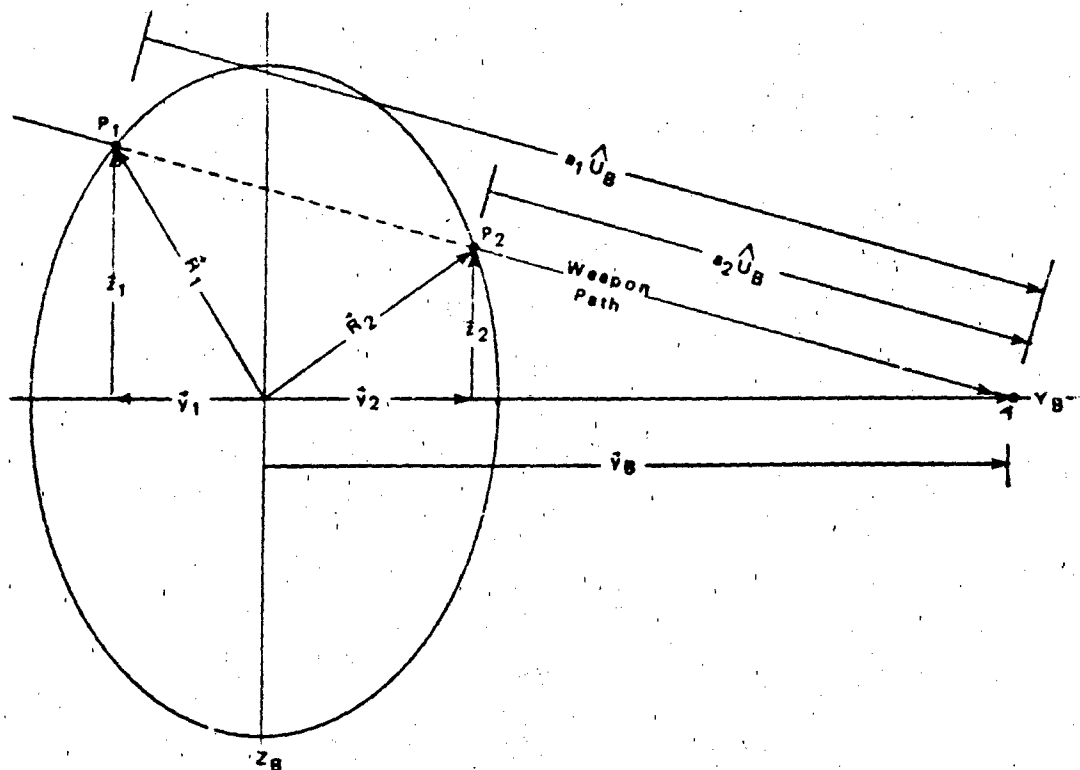


Figure 4. End View of Penetrated Ellipsoid

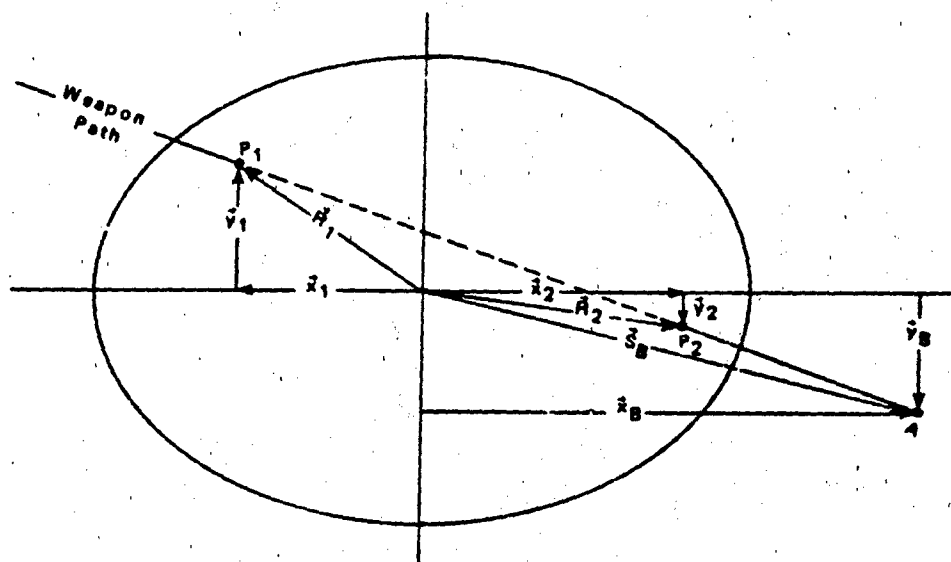


Figure 5. Top View of Penetrated Ellipsoid

where:

$$A = \cos^2 \theta \cos^2 \psi (\beta\gamma)^2 + \cos^2 \theta \sin^2 \psi (\alpha\gamma)^2 + \sin^2 \theta (\alpha\beta)^2 \quad (30)$$

$$B = 2(\alpha\gamma)^2 \cos \theta \sin \psi y_B - 2(\beta\gamma)^2 \cos \theta \cos \psi x_B \quad (31)$$

$$C = (\beta\gamma)^2 x_B^2 + (\alpha\gamma)^2 y_B^2 - (\alpha\beta\gamma)^2 \quad (32)$$

Two values of  $a$ , i.e.  $a_1$  and  $a_2$ , are found by this method corresponding to points  $P_1$  and  $P_2$ . If  $\theta > 0$ , then  $z_1 < z_2$  and:

$$a_1 = -\frac{B}{2A} + \left| \frac{\sqrt{B^2 - 4AC}}{2A} \right| \quad (33)^*$$

$$a_2 = -\frac{B}{2A} - \left| \frac{\sqrt{B^2 - 4AC}}{2A} \right| \quad (34)^*$$

otherwise, for  $\theta < 0$ , the values of  $a_1$  and  $a_2$  in Equations (33) and (34) are interchanged. The components  $x_1$ ,  $y_1$ ,  $z_1$ , and  $x_2$ ,  $y_2$ ,  $z_2$  can be found from Equations (24), (25) and (26).

Then, from Figures (4) and (5) it can be seen that:

$$\vec{R}_1 = x_1 \hat{i} + y_1 \hat{j} + z_1 \hat{k} \quad (35)$$

$$\vec{R}_2 = x_2 \hat{i} + y_2 \hat{j} + z_2 \hat{k} \quad (36)$$

The total length of the path within the ellipsoid  $L$  is:

---

\* Absolute values in Equations (33) and (34) are required to identify the entry and exit points in the ellipsoid.

$$L = |\vec{R}_1 - \vec{R}_2| = |a_2 - a_1| = \left| \frac{\sqrt{B^2 - 4AC}}{A} \right| \quad (37)$$

A question may be raised at this time about what would happen if  $S_B$  fell within the ellipsoid. In this case, the signs of  $a_1$  and  $a_2$  would differ and Equation (24), (25) and (26) would still remain valid. There would therefore be no change in the solution.

The solution of the path of the weapon within the body also involves, by definition, a solution for the angles of impact and exit which the weapon makes with the target body [see Figure (6)]. This solution can easily be found from the equation of the surface  $\Phi$ , the gradient  $\vec{\nabla}\Phi$  will be a vector perpendicular to the surface at  $(x_i, y_i, z_i)$ . For an ellipsoid, it can therefore be stated:

$$\vec{\nabla}\Phi = \frac{2x_i}{a^2} \hat{i} + \frac{2y_i}{b^2} \hat{j} + \frac{2z_i}{c^2} \hat{k} \quad (38)$$

where  $i = 1$  for impact and  $i = 2$  for exit. A unit vector  $N$  can be formed in the direction of the gradient:

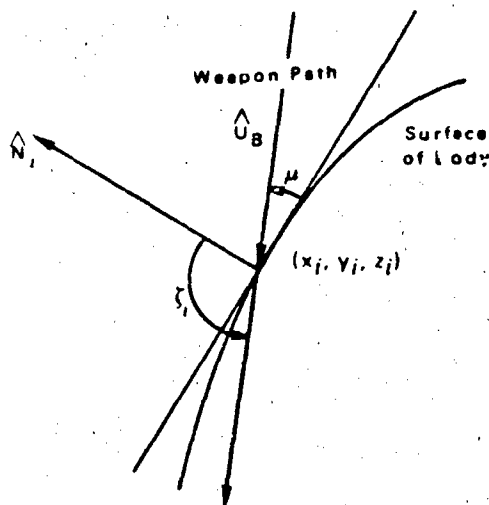


Figure 6. Impact Angle to Target Surface

$$\hat{N}_i = \frac{\vec{\nabla}\Phi}{|\vec{\nabla}\Phi|} = \frac{(\beta\gamma)^2 x_i \hat{i} + (\alpha\gamma)^2 y_i \hat{j} + (\alpha\beta)^2 z_i \hat{k}}{\sqrt{(\beta\gamma)^4 x_i^2 + (\alpha\gamma)^4 y_i^2 + (\alpha\beta)^4 z_i^2}} \quad (39)$$

and from the definition of the dot product between two vectors:

$$\hat{N}_i \cdot \hat{U}_B = |\hat{N}| |\hat{U}_B| \cos \zeta_i \quad (40)$$

where  $|\hat{N}| = 1$ ,  $|\hat{U}_B| = 1$ :

$$\frac{\hat{N} \cdot \hat{U}_B}{|\hat{N}| |\hat{U}_B|} = \cos \zeta_i = \frac{(\beta\gamma)^2 x_i \hat{i} + (\alpha\gamma)^2 y_i \hat{j} + (\alpha\beta)^2 z_i \hat{k}}{\sqrt{(\beta\gamma)^4 x_i^2 + (\alpha\gamma)^4 y_i^2 + (\alpha\beta)^4 z_i^2}} (x_u \hat{i} + y_u \hat{j} + z_u \hat{k}) \quad (41)$$

Because:

$$\mu_1 = \zeta_1 - \frac{\pi}{2} \quad (42)$$

$$\mu_2 = \frac{\pi}{2} - \zeta_2 \quad (43)$$

where  $\mu_1$ , and  $\mu_2$  are the impact and exit angle, respectively, formed by the weapon trajectory with the target surface (see Figure 6). Then the impact angle:

$$\mu_1 = \sin^{-1} \frac{D}{E} \quad (44)$$

where:

$$D = (\alpha\gamma)^2 \cos \theta \sin \psi y_i - (\beta\gamma)^2 \cos \theta \cos \psi x_i - (\alpha\beta)^2 \sin \theta z_i \quad (45)$$

$$E = \sqrt{(\beta\gamma)^4 x_i^2 + (\alpha\gamma)^4 y_i^2 + (\alpha\beta)^4 z_i^2} \quad (46)$$

and the exit angle:

$$\mu_2 = \sin^{-1} \frac{F}{G} \quad (47)$$

where:

$$F = (\alpha\beta)^2 \sin \theta z_2 + (\alpha\beta)^2 \cos \theta \sin \psi y_2 + (\beta\gamma)^2 \cos \theta \cos \psi x_2 \quad (48)$$

$$G = \sqrt{(\beta\gamma)^4 x_2^2 + (\alpha\gamma)^4 y_2^2 + (\alpha\beta)^4 z_2^2} \quad (49)$$

### Planar Surface Fitting Models

Perhaps the most realistic and practical methods for obtaining a mathematical description of a physical target configuration for endgame direct hit effectiveness analysis programs is the methodology presently used in defining target vulnerability data for fragmentation and other penetration kill mechanisms. This methodology, as typified by the computer simulation programs SHOTGEN (References 27 and 28), and TARGET DESCRIPTION (Reference 29) uses planar surface approximations for fitting actual physical configurations and can be made as accurate as desired by using more or fewer surfaces or points defining the surface vertices.

SHOTGEN uses a series of sequential points such that the third and each succeeding point complete the definition of a triangle whose vertices are the last three points in the sequence. By double-pointing or using the same point twice in the sequence, a degenerate triangle or straight line is defined. The surface of any object, however complex, can be approximated in this manner with the degree of accuracy dependent on the number of points defined. The more complex the physical shape, the more points are required for a given level of accuracy. Figure 7 illustrates a target defined by this method.

TARGET DESCRIPTION uses both quadrilateral or triangular planar input to approximate actual physical shapes in much the same manner as SHOTGEN. It has no advantage in accuracy since any quadrilateral can be formed from two triangles. The only difference is in the facility for input. The TARGET DESCRIPTION program permits

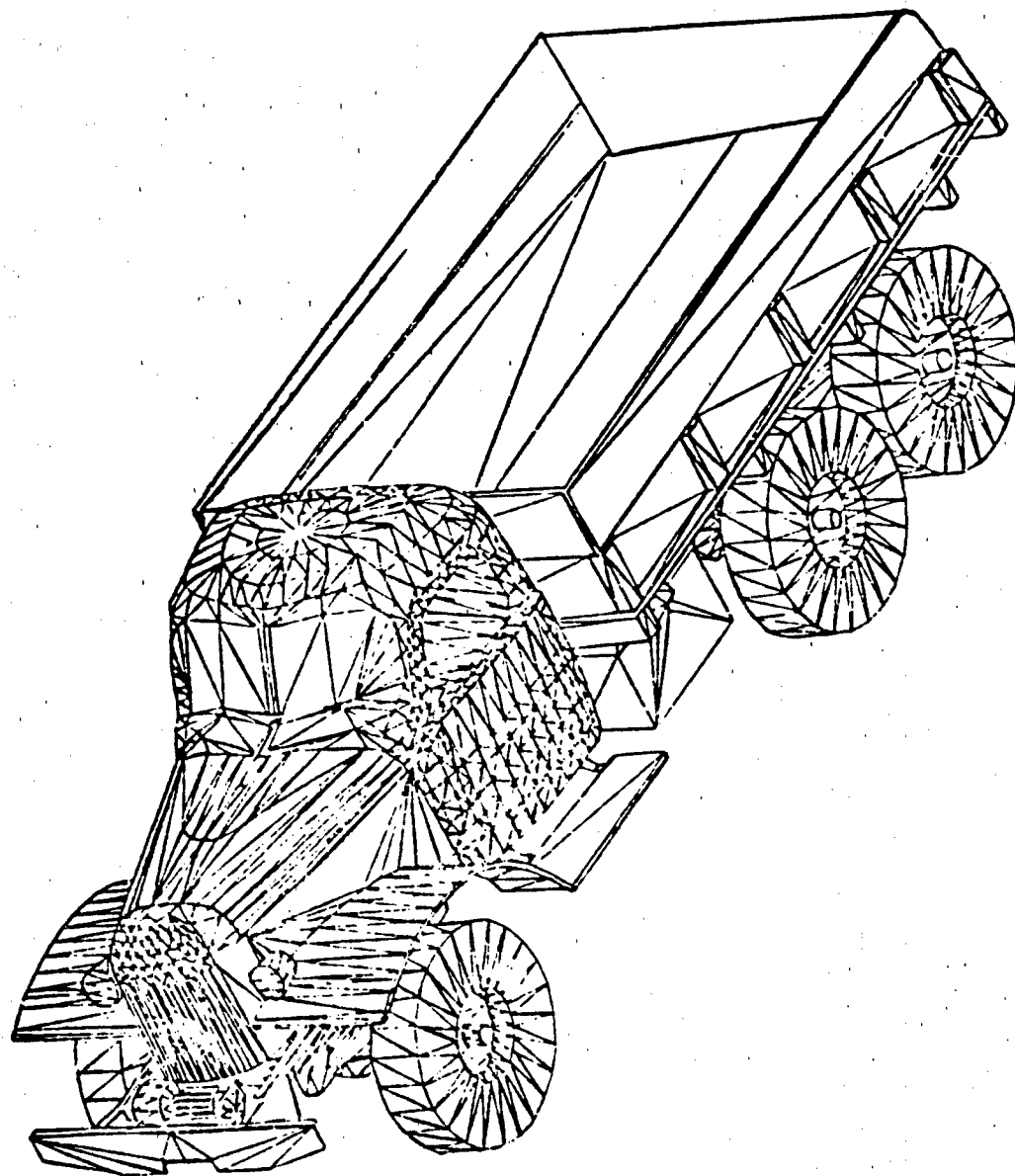


Figure 7. SHOTGEN Model

input of common figures such as boxes, cylinders, cones, pyramids, wedges, etc., with minimal input. The program automatically breaks down the standard figure to quadrilateral or triangular approximations and computes all the vertices. Again, any degree of accuracy can be attained if enough points are used. An example is shown in Figure 8.

Another program which performs a very adequate function of simulating target physical configurations is the COMGEOM (combinatorial geometry) program which defines the input for the MAGIC target vulnerability program (References 30 and 31). This program uses a combination of standard planar figures (parallelepipeds, pyramids, or polyhedrons of 4, 5, or 6 faces) and the quadric surface figures, and can even define arbitrarily curved surfaces. An example of a tank target described in this manner is shown in Figure 9.

Any of the above three programs can achieve excellent target physical simulation for direct hit evaluation and should be considered for future development of computer programs for effectiveness analysis of terminally guided air-to-surface and surface-to-surface weapon systems.

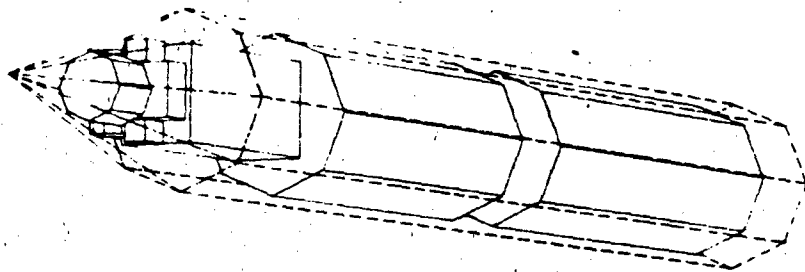


Figure 8. TARGET DESCRIPTION Model.

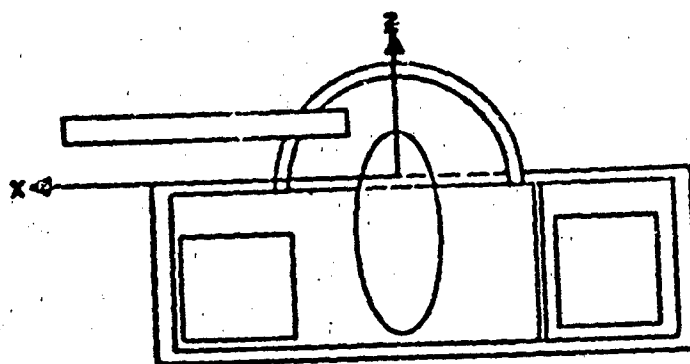
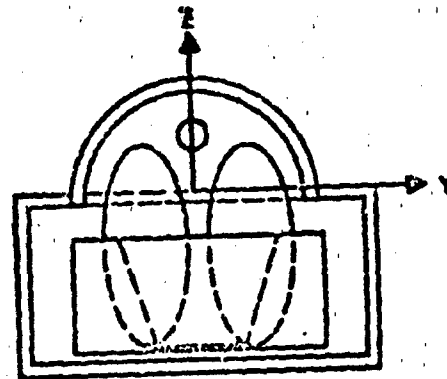
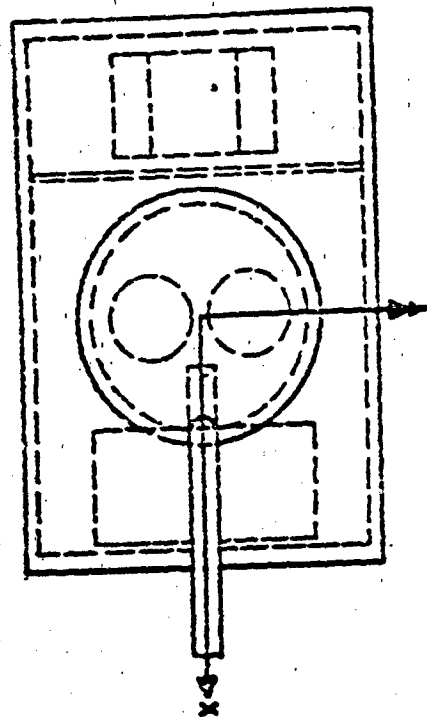


Figure 9. COMGEOM Model



## SECTION III

### BLAST DAMAGE VULNERABILITY SIMULATION MODELS

#### BLAST DAMAGE EFFECTIVENESS INDICES

To evaluate blast kill mechanisms against various target element types or against target complexes, four EIs have been defined:

- Mean Effective Diameter (or Lethal Radius)
- Crater Diameter
- Effective Miss Distance (EMD)
- Blast Mean Area of Effectiveness (MAE<sub>b</sub>)

The first EI, Mean Effective Diameter, is used to determine the effectiveness of mines (see References 32 through 41). It is defined as the diameter of a circle, centered at the mine body, within which a finite probability of mine actuation and subsequent blast damage to a target element exists. This EI (interchangeably used or referred to as Lethal Radius) is sometimes erroneously used for the evaluation of fragmenting mines or active air delivered munitions. In this usage, the combined blast and fragmentation kill mechanism effects are used to define the Mean Effective Diameter, or Lethal Radius, and a rough estimate of effectiveness is based on probability of weapon detonation within the defined circular boundary. Computer programs using this EI are statistically optimistic in that the kill probability predictions are greater than with other (more accurate) methods.

Crater diameter is used primarily for linear targets such as roads, railroad tracks or airfield runways. In these instances, the usable width of the road, track, or runway must be sufficiently cut by the crater or by adjacent craters such that passage is denied to traffic.

The Effective Miss Distance (EMD) of a target is defined as the maximum distance from the target edge or surface at which the weapon can be detonated and still inflict the desired damage. Calculations which consider EMD as the EI normally require that the area or volume around the target enclosed by the EMD be treated exactly as if it were part of the target.

Blast Mean Area of Effectiveness ( $MAE_b$ ) is a casualty or damage effectiveness index which is often approximated by a circular pattern. The probability of damage given a hit ( $P_{HD}$ ) within the circular pattern radius is unity, and beyond that distance,  $P_{HD}$  is zero. The concept of  $MAE_b$  is not used for three-dimensional simulation. Mathematically, the magnitude of  $MAE_b$  is computed by the formula:

$$MAE_b = \int_0^{2\pi} \int_0^R P_{KB}(r, \theta) r dr d\theta \quad (50)$$

Where  $P_{KB}(r, \theta)$  is the probability of obtaining a kill due to blast damage at a distance  $r$  and azimuth angle  $\theta$  from the weapon to the target centroid ( $r$  and  $\theta$  are measured in the ground plane), and  $R$  is a distance beyond which  $P_{KB}$  is zero for all azimuth angles. Physically, the concept of a circular area for representing  $MAE_b$  is usually an adequate simulation technique for evaluation of weapon system blast lethality whenever the target is small with respect to  $MAE_b$  and impact detonating fuzes are used. This is so because blast effects are nearly spherical in their volume of influence and because the difference between the distance at which 100 percent blast kill is achieved and the distance at which no kill can be expected is relatively small for a large range of target types.

## BLAST PHYSICAL SIMULATION MODELS

Most physical simulation models for blast lethality are relatively simple in nature compared to direct hit or fragmentation kill models. The simplest of these are, of course, the two-dimensional models. There are also more realistic three-dimensional blast models which are functionally dependent on distance, and a few in which corrections for atmosphere and other dependent variables are made.

### Two-Dimensional Models

Two-dimensional blast damage simulation models are usually extensions of direct hit models, if they co-exist in the same program, and are simply concentric similar figures. If the direct hit physical dimensions are modeled by a rectangle, the blast model is merely a slightly larger rectangle with both the length and width dimensions increased by an effective miss distance (EMD) (References 42 through 45).

If the evaluation model ignores the possibility of direct hit kill, the oversight is normally corrected by means of the blast kill formulation. The rationale is usually that all direct hits would be well within the lethal blast radius and would therefore be scored as a kill by blast. This type of two-dimensional blast model is consistent with the general approach to keep evaluation programs simple and efficient; however, for targets where direct hit is a critical kill mechanism (bunkers, tanks, armored personnel carriers, etc.), the simple approach does not provide the required accuracy, especially for terminally guided munitions, low angle delivery, or direct fire weapons. If the direction from which the weapon approaches the target can be considered to be always parallel or perpendicular to the rectangular target area, then for a two-dimensional target (i.e., a target without height), the effective target length ( $L_{ET}$ ), effective target width ( $W_{ET}$ ), and effective target area ( $A_{ET}$ ) are defined as:

$$L_{ET} = L_T + 2EMD \quad (51)$$

$$W_{ET} = W_T + 2EMD \quad (52)$$

$$A_{ET} = (L_{ET})(W_{ET}) \quad (53)$$

where  $L_T$  is the dimension of the target parallel to the flight path and  $W_T$  is the dimension of the target perpendicular to the flight path. For example, the target shown in Figure 10 has a target length of 50 feet and a target width of 40 feet. If the EMD is 10 feet, then  $L_{ET}$  would be 70 feet,  $W_{ET}$  would be 60 feet and  $A_{ET}$  would be 4,200 square feet.

For a three-dimensional target and an impact detonating fuze, the effective two-dimensional target area is a composite of the plan target area, the area around the target defined by the EMD, and the shadow area resulting from the projection of the target in the ground plane, as shown in Figure 11. The shadow length is:

$$L_{SH} = \frac{H_T}{\tan i} \quad (54)$$

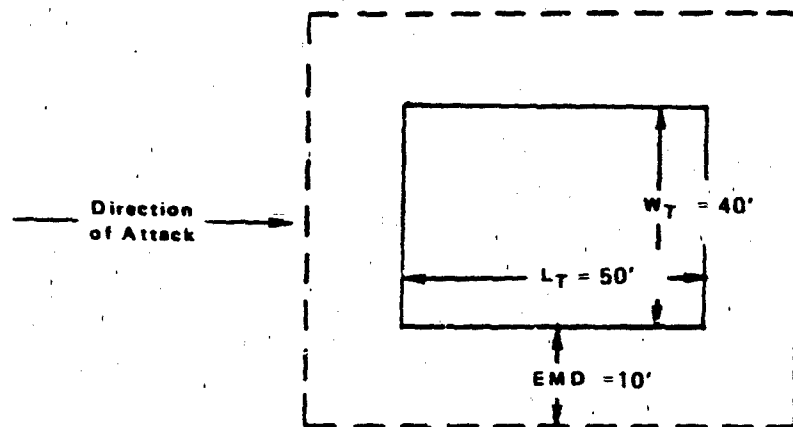


Figure 10. Effective Miss Distance About a Rectangular Target

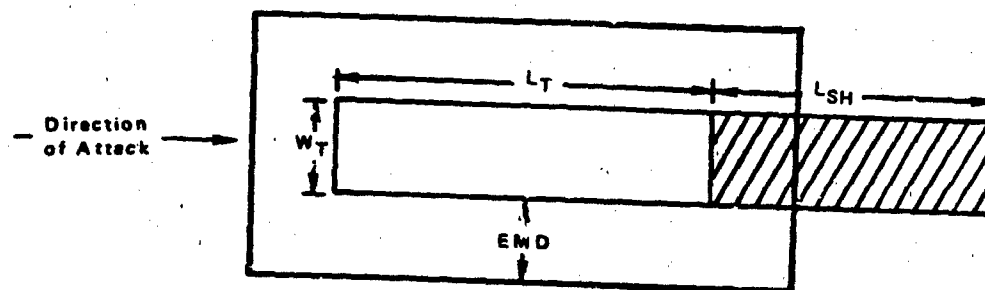


Figure 11. Effective Target Area

where  $I$  is the impact angle and  $H_T$  is the height of the target. The effective target area is thus:

$$A_{ET} = (L_T + 2EMD)(W_T + 2EMD) + W_T(L_{SH} - EMD) \quad (55)$$

To obtain the effective target length ( $L_{ET}$ ) and effective target width ( $W_{ET}$ ), it is sufficient to convert the above irregular projected area into an equivalent rectangular area with the width  $W_{ET} = W_T + 2EMD$ .  $L_{ET}$  is thus defined as:

$$L_{ET} = \frac{(L_T + 2EMD)(W_T + 2EMD) + W_T(L_{SH} - EMD)}{W_{ET}} \quad (56)$$

If the target requires a single direct hit to produce the desired blast damage EMD is zero.

For air burst or proximity fuzes it is necessary to include the effective target height ( $H_{ET}$ ) directly rather than its projection into the ground plane (shadow effect), since the lethal blast radius is truly three-dimensional. The pseudo three-dimensional technique of including the shadow area of the target to determine hit probability of a three-dimensional object in two-dimensions is therefore inaccurate for an air blast damage mechanism evaluation model.

When the  $MAE_b$  is used as an EI, the effective target length  $L_{ET}$  and effective target width  $W_{ET}$  may be defined as:

$$L_{ET} = W_{ET} = \sqrt{MAE_b} \quad (57)$$

The evaluation is always two-dimensional in this event since  $MAE_b$  is defined as a two-dimensional EI.

### Three-Dimensional Models

The second level of sophistication in blast damage evaluation models is the three-dimensional blast volume, within which blast kill is a

certainty and for which external detonation cannot produce a blast kill. Nearly one-half of the programs which contain three-dimensional blast models use a simple sphere to model a lethal blast radius around the target, and most of the remainder use a parallelepiped. Only a very few permit the use of ellipsoids or cylinders, and none of those reviewed contained more exotic conic sections or quadric surface models. Figure 12 is an example of an ellipsoidal blast envelope about a parallelepiped (box) target element. This model is a more realistic simulation of blast vulnerability than using a larger box to define the blast surfaces.

Although the target description and vulnerability programs, SHOTGEN, COMGEOM, and TARGET DESCRIPTION, are concerned with describing the physical target and not a lethal blast envelope, a logical extension of this more sophisticated methodology could be applied to blast damage evaluation. This would require that each of the planar or quadric surfaces be projected from a single interior point such that a larger similar physical model is defined at the effective miss distance from the original surfaces. An example of a good three-dimensional blast model is given in AFATL's aircraft shelter vulnerability computer program documented in Reference 46. This program contains an excellent description of blast damage evaluation methodology which is typical of that contained in the better three-dimensional blast lethality evaluation models.

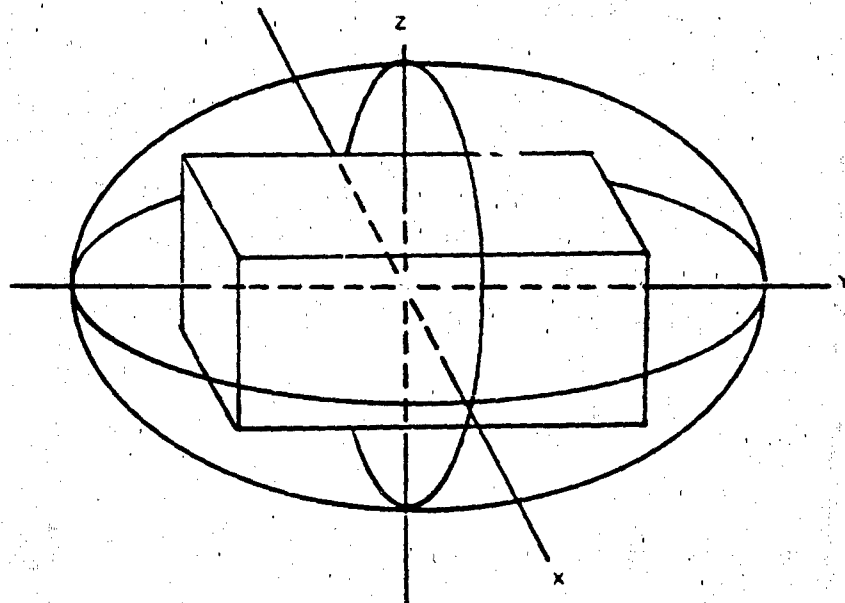


Figure 12. Blast Ellipsoid Around Box-Shaped Target

### Blast Damage as a Function of Distance

The next level of sophistication of blast models is the definition of variable blast kill as a function of distance. This method always can be reduced to the basic concept of two blast envelopes. The inner envelope represents the maximum (usually 100 percent) kill boundary, and the outer envelope represents the boundary beyond which blast kill is always zero. Between the two envelopes, some form of mathematical interpolation technique defines the probability of obtaining a blast kill. Almost invariably the interpolation techniques are linear, although the physics of blast impulse would suggest that interpolation according to the inverse square or cube of the distance, or a logarithmic technique would be more accurate.

To illustrate the mathematics of such a model, consider a simple point target with blast envelopes modeled as spheres. Two radial distances are input directly or calculated from input values of target critical impulse levels and warhead equivalent bare charge weight of explosive. Let  $R_{B1}$  and  $R_{B2}$  denote these distances as shown in Figure 13 and interpolation be linear.

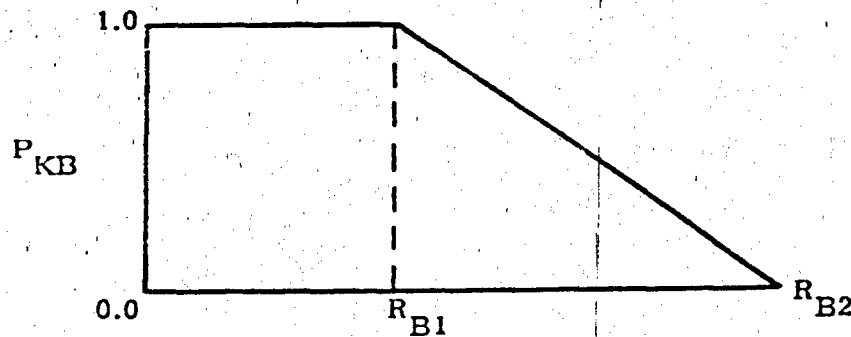


Figure 13. Probability of Blast Kill Versus Distance

Then the kill probability due to blast,  $P_{KB}$ , is given by the following relation:

$$P_{KB} = \begin{cases} 1 & \text{for } 0 < D < R_{g1} \\ \frac{R_{B2} - D}{R_{B2} - R_{B1}} & \text{for } R_{B1} < D < R_{B2} \\ 0 & \text{for } D > R_{B2} \end{cases} \quad (58)$$

where D is the distance from the warhead to the target. An example of this methodology as used in a two-dimensional model for evaluating Lethal Area is contained in Reference 14.

#### Atmosphere and Other Variable Dependent Models

Blast model evaluation methodology in the most sophisticated programs provides corrections to the size of computed blast envelopes as functions of kinematic encounter variables such as atmospheric pressure at the target due to altitude above sea level or meteorological changes in the environment, or azimuth and elevation angle of the approaching blast wave. Since blast impulse propagation is a mass-transfer wave phenomena, the acoustic properties of the transfer medium determine the amount of energy transfer. Thus, a given weight of explosive will transmit energy better through a denser medium; therefore, high atmospheric pressure and moisture content will support greater target damage than a low pressure, dry environment, all other things being equal. Since air density varies with altitude above sea level in approximately the ratio  $\frac{1}{8}$  for each 31,000-foot change in altitude, the blast impulse I should include a multiplicative correction of:

$$I = I_{SL} e^{\frac{H}{31000}} \quad (59)$$

where  $I_{SL}$  is the computed impulse at sea level and H is the target height (altitude) above sea level. The JMEM/AS open end methods for the Wang computer (Reference 17) contains the correction.

Corrections to lethal blast radii for direction of approach of the blast wave are desirable for realistic blast damage probability prediction.



For example, a large radar or electronics van (defined as a parallelepiped) would be more vulnerable to blast impulse impinging broadside upon a large surface area than to the same blast impulse impinging upon the ends or corners of the van. The concept of effective miss distance cannot be wholly accurate, therefore, without variation as a function of relative aspect angles from which the blast wave approaches the target. Except for the methods using blast ellipsoids, this correction was not found in any of the air-to-surface programs examined.

Finally, a point which is almost universally ignored for computing blast kill in air-to-surface effectiveness programs is the terminal velocity of the weapon at detonation and the effect this has on the formation and propagation of the blast wavefront. This effect is perhaps of minor significance for impact detonated munitions since the primary shock wave comes from a reinforced Y stem effect due to reflection of the blast wave from the ground or other surface. For influence and proximity fuze weapons, however, it is of major importance in computing the magnitude of an incident blast wave to know if a missile is approaching or receding from the target at the time of detonation. In most, if not all, surface target effectiveness programs, these kinematic influences are not considered.

## SECTION IV

### FRAGMENTATION DAMAGE EFFECTIVENESS METHODOLOGY

#### FRAGMENTATION DAMAGE EFFECTIVENESS INDICES

There are only two EIs which are used for evaluation of fragmentation weapon lethality — Mean Area of Effectiveness and Vulnerable Area; both have been discussed in previous sections. However, since evaluation of fragmentation kill is often the most difficult and important task of the weapons analyst, it is considered desirable to develop these concepts further for this section.

A frank discussion of fragmentation Mean Area of Effectiveness ( $MAE_f$ ) should begin with a strong statement to "BEWARE" in the use of this EI. Unlike  $MAE_b$ , there is very little in the way of physical realism or tangible simulation concepts which can be attributed to  $MAE_f$ . As a comparison tool, the concept of MAE is a very utilitarian measure of effectiveness. Problems invariably arise, however, whenever  $MAE_f$  is converted to a more universally understood (or accepted) concept, single shot probability of damage ( $SSP_D$ ) [or single shot kill probability ( $P_{KSS}$ )].  $MAE_f$  is a casualty or damage index which is related to the average number of target elements damaged by a weapon when the target elements (e.g., personnel) are assumed to be uniformly distributed over the target area. If targets are uniformly distributed over an area with a fixed density of targets per unit area, then  $MAE_f$  represents the expected number of targets damaged (e.g., expected number of personnel casualties).  $MAE_f$  depends upon the target vulnerability, weapon characteristics, impact velocity, weapon angle of fall, and burst height. For evaluating weapon effectiveness against a single target element or other than a uniform distribution of target elements, care must be taken to insure that the techniques for averaging effects of  $MAE_f$  do not negate the applicability of the methodology for the given weapon system.  $MAE_f$  should never be used for  $SSP_D$  evaluation of directional or focused fragmentation munitions or conventional cylindrical weapons with low impact angles against finite target elements.

In the JMEM open end methodology, for the purpose of computation, MAE for a weapon/target combination is the area over which a weapon, on the average, will cause at least the specified damage to particular target elements. Since the effects for bombs and missiles are more elliptical than circular, an additional factor needed for computations is

the length-to-width ratio ( $a$ ) which can be used to provide a closer approximation to the shape of the damage pattern. To determine effectiveness parameters for this EI, an ellipse is obtained whose area is  $MAE_f$  and whose ratio of minor to major axis is ( $a$ ). The effective target length ( $L_{ET}$ ), effective target width ( $W_{ET}$ ), and effective target area ( $A_{ET}$ ) are therefore defined as:

$$L_{ET} = 2 \sqrt{\frac{MAE_f(a)}{\pi}} \text{ or } 1.128 \sqrt{MAE_f(a)} \quad (60)$$

$$W_{ET} = \frac{L_{ET}}{(a)} \quad (61)$$

$$A_{ET} = MAE_f \quad (62)$$

If  $a$  is nearly one (i.e., the impact angle is near 90 degrees), then the pattern will be nearly circular in shape, and:

$$L_{ET} = W_{ET} = 2 \sqrt{\frac{MAE_f}{\pi}} \quad (63)$$

The mathematical definition of  $MAE_f$  is:

$$MAE_f = \int_0^{2\pi} \int_0^R P_{KF}(r, \theta) r dr d\theta \quad (64)$$

where  $P_{KF}(r, \theta)$  is the probability of obtaining a kill due to fragmentation damage at a distance  $r$  and azimuth angle  $\theta$  from the weapon to the target centroid. A similar formula for  $MAE_b$  was given in Section III with little or no qualification for its use. The difference in the defining functions  $P_{KB}$  versus  $P_{KF}$  is important and must be understood to permit proper use of the concepts.

As stated before, for nearly all conventional weapons containing high-explosive chemicals, blast effects are nearly spherical (highly symmetric) in their realm of influence. The  $P_K$  function is therefore independent of azimuth angle  $\theta$ . Also, for most targets a sharply defined blast damage threshold exists, which means that the  $P_K$  function is unity

within a threshold radius and drops rapidly to zero outside this radius.

The fragmentation kill probability function ( $P_{KF}$ ) is not nearly so well behaved. First of all, except for spherical munitions or cylindrical munitions delivered at 90° elevation, the function is highly  $\theta$  dependent. Also, there is nothing continuous about a fragmentation pattern composed of a finite number of fragments, and since fragments can maintain a lethal velocity over a long range, the limit of integration  $R$  is a relatively long distance from the detonation point origin. To summarize, the complexity of the  $P_{KF}$  function and its discontinuous nature make it unsuited to the type of averaging calculations associated with MAE. The result is a tendency to overestimate  $SSP_D$ . Given any particular weapon system, the standard computational practice of assuming a lethal radius given by:

$$R_L = \sqrt{\frac{MAE_f}{r}} \quad (65)$$

will normally result in an over estimation of  $SSP_D$ .

The other fragmentation effectiveness index, vulnerable area (VA), is that portion of the target presented area which is vulnerable to an individual fragment. The VA is therefore a function of individual fragment parameters (weight, shape, and striking velocity) as well as the aspect angles (azimuth and elevation) at which the fragment strikes the target. VA is a more basic entity than MAE and, in fact, must be used in the computation of MAE.  $SSP_D$  for fragmentation can also be calculated directly from VA, and although the integration is more complicated, the results are more accurate.

Perhaps the best way to define this EI is to give a short description of the methodology for computing VA using the computer programs SHOTGEN or MAGIC. These programs produce the data to compute target vulnerable areas as a function of fragment classes (which are determined by a unique striking mass (size and shape) and as a function of striking velocity and aspect angles (azimuth and elevation).

Target vulnerability is described in terms of the vulnerable component concept. The substructures of the target that are most essential to the target's continued usefulness, and which cannot be immediately

repaired if damaged, are considered to be vulnerable components. For example, if the target is a truck, the engine, transmission, fuel tanks, ignition system, coolant system, electrical system, suspension, and possibly the driver may be considered as vulnerable components. The assigned level of damage probability given a hit ( $P_{HD}$ ) is specified for each vulnerable component and each fragment class.

The amount of metal that an incoming fragment must penetrate to reach a vulnerable component may vary greatly with the weapon's direction of approach. For example, a fragment approaching a voltage regulator from above might encounter a small fraction of an inch of shielding, while a fragment approaching from the front or rear might have to penetrate several inches of metal before reaching the regulator. The problem is that nothing is known in advance about the orientation of the target with respect to the weapon burst point; therefore, a specific direction of fragment approach to a vulnerable component cannot be specified. At first consideration it would seem reasonable to look at the components in question from every angle, average the encountered metal thicknesses, and consider this as the shielding. The procedure has at least one constraint: a weapon may have a penetrating threshold below this average thickness. Therefore, we would calculate a zero probability of kill for this weapon even if the weapon can, in reality, penetrate the component shielding from certain aspects.

The SHOTGEN and MAGIC programs solve the above difficulty by computing the shielding thicknesses for each component at prescribed azimuth and elevation viewing aspects. The programs set up a grid in space which is normal to a ray corresponding to a particular viewing aspect. Fragment projectile lines (shotlines), which are normal to and randomly located within each cell of the grid, are projected toward the target (as shown in Figure 14). Each of these lines is examined in turn to determine which of the target components is encountered along the shotline. The sequence in which component is encountered and the equivalent material thicknesses are then stored on a magnetic tape for future processing. The smaller the individual grid size, the greater the accuracy, and also the greater the computer time required to compute all the shotline data for a given viewing aspect. Increased accuracy can also be obtained from an increased number of viewing aspects at the expense of computer running time.

After the individual shotline data has been collected, it is processed by a vulnerability program such as VAREA (Reference 47). Besides the shotline data, the individual values of fragment classes and initial striking

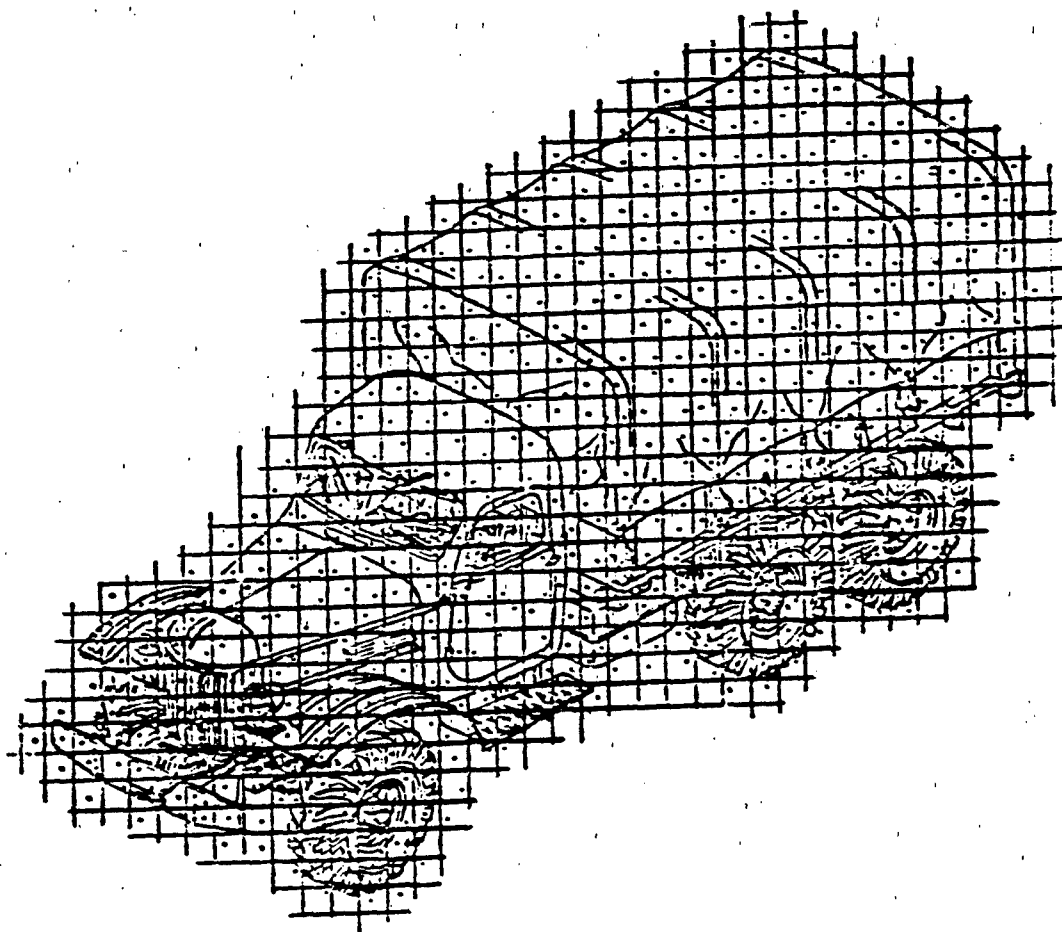


Figure 14. SHOTLINE Grid

velocities must be specified. Each of the shotlines are examined for each target component in the sequence in which they are encountered and for each fragment class and initial striking velocity. This is done to establish whether a penetration into a vulnerable component takes place. Penetration is determined with the use of equations (Reference 48) which predict residual mass and velocity for fragments impacting specified thicknesses of target materials. If the shotline does not intersect a vulnerable component or the fragment does not have sufficient mass or velocity to penetrate to the component, then no vulnerable area is

accumulated for that shotline. For each fragment that does penetrate a vulnerable component, the cell area in the original grid is multiplied by an appropriate  $P_{HD}$  and accumulated as a minute bit of vulnerable area. By collecting the vulnerable area accumulated at each variable increment, vulnerable area tables are produced which tabulate the data in terms of azimuth and elevation angles, and fragment weights and velocities. The above programs also produce tables of average vulnerable area for individual components or for the entire target. This may be accomplished by averaging over all possible azimuths at a particular elevation angle. The table is then indexed by elevation angle for all elevation angles of concern.

## FRAGMENTATION PHYSICAL SIMULATION MODELS

All fragmentation effectiveness analysis models which use  $MAE_f$  as an input effectiveness index are statistical models which operate in the same manner as for  $MAE_b$ . These models are efficient closed form type programs and are useful for obtaining preliminary estimates, processing large amounts of parametric data, or conserving effort and computer time when absolute accuracy is not critical. Examples of two of the better methodologies of this type are given in References 49 and 50.

All other fragmentation evaluation programs, including those which compute the input values of  $MAE_f$  for individual weapons, use VA as an effectiveness index and all are basically identical in the methodology for computation of  $P_{SSK}$  (or  $SSPD$ ). An example of this methodology follows.

### Fragmenting Munition Effectiveness Analysis

Target input data for evaluating fragmenting munitions consists of tables of vulnerable areas as functions of fragment striking velocities, mass, and aspect angles, as previously defined. The more sophisticated models will accept larger arrays representing finer detail in the vulnerability model, and they usually will provide for simultaneous evaluation of several types of targets and many locations for each type.

The fragmentation characteristics of a warhead are defined in terms of polar zones bounded by polar angles measured from the nose of the warhead. Most programs assume symmetry about the longitudinal axis, but the more sophisticated programs allow also for variation in fragmentation characteristics in longitudinal angular zones as well. Warhead performance is input in tabular form for one or more classes of

fragments each having a unique initial velocity, weight, and presented area. The tables also define the number of fragments of each class which are ejected from each zone (defined by upper and lower polar angles and, if applicable, upper and lower longitudinal angles).

Other inputs include the terminal delivery conditions such as weapon system approach azimuths, dive angles, deployment altitude, number of munitions delivered in a single pass, delivery errors, ballistic errors, submunition distribution, and submunition terminal velocities. The most sophisticated programs have fuzing options for altimeter fuzes, active or passive radar fuzes, slant range fuzes, electro-optical fuzes and other influence fuzes, as well as impact and delayed detonation fuzes. For target complexes containing more than one type of vulnerable component, there must also be kill criteria specified to determine which and how many components must be damaged to constitute a kill of the entire target complex.

Programs using the Monte Carlo procedure select a random sample of detonation points for each munition in a single pass and evaluate the probability of killing each target component with fragments projected from each detonation point. This process is repeated many (several hundred) times to obtain average kill probabilities for killing each component in a single pass, and the probabilities are then combined to obtain the single shot kill probability for the entire complex according to the stated kill criteria.

Other integration techniques are available which define specific evaluation points in terms of standard deviations. For each such point, a distribution weighting factor is also specified which represents a probability that a variable will be found within an interval with boundaries between the two adjacent evaluation points. For comparison evaluations where only one or two variables are involved in the integration, these fixed tabular integration techniques are generally superior in accuracy and efficiency. For three or more variables, the random number technique is equal in accuracy and efficiency and considered by many to represent a more realistic simulation of the truly random nature of weapons delivery processes.

The mathematical expression defining fragmentation kill probability for a single weapon, according to the Binomial Distribution Theorem, is:



$$P_{KF} = 1 - \prod_{k=1}^{N_c} \left(1 - \frac{Av_k}{A_p}\right)^{N_k} \quad (66)$$

where  $N_c$  is the number of fragment classes from the warhead which strike the target,  $A_p$  is the total presented area of the target exposed to the fragment hits,  $Av_k$  is the area which is vulnerable to the  $k^{th}$  class of fragments, and  $N_k$  is the number of fragments of class  $k$  which strike the target. By making logical simplifying assumptions that the distribution of fragments within each class is uniform over a given polar (and longitudinal) zone and that the Poisson approximation to the Binomial Equation is valid, a simpler form of the basic expression defining  $P_{KF}$  is assumed to be:

$$P_{KF} = 1 - \exp \left[ - \sum_{k=1}^{N_c} \rho_k Av_k \right] \quad (67)$$

where  $\rho_k$  is the spatial density of fragments from the  $k^{th}$  class striking the target (i.e.,  $\rho_k = N_k/A_p$ ). If the target under consideration is personnel, the  $Av_k$  defined as follows:

$$Av_k = (A_p) (P_{ck}) \quad (68)$$

where  $A_p$  is the target presented area as a function of height of burst and horizontal distance, and  $P_{ck}$  is the kill probability based on a fragment hit of a certain mass and velocity. The presented areas for standing, prone, and foxholed troops in various types of terrain as defined by the Ballistic Research Laboratories (BRL) may be input or compiled into the programs. The BRL conditional kill probability expression (Reference 51) is used to compute  $P_{ck}$ .

To evaluate Equation (67) the following information must be determined:

- Each class of fragments from the warhead which strike the target
- Striking velocity of the fragments of each class
- Striking aspect angles of the fragments of each class
- Striking density of the fragments of each class.

Some programs assume a static situation (i.e., that the warhead is on the ground and stationary at the time of detonation), but the more accurate programs calculate relative velocities and dynamic fragment characteristics. The dynamic fragmentation characteristics are obtained by vectoring the static warhead fragmentation data forward with respect to the missile velocity vector. Hence, each static class of each polar zone is redefined to form a new dynamic fragment class with its own upper and lower polar angle limits.

These dynamic polar angle limits for each class of fragments are used in conjunction with the following relations to determine which of these classes have fragments that strike the target at the point location  $(x_T, y_T, z_T)$  under consideration. The angle from which a fragment must emerge to strike the target is given by:

$$\phi = \cos^{-1} \left[ \left( \frac{x_T - x_w}{D} \right) \cos \alpha \cos \theta + \left( \frac{y_T - y_w}{D} \right) \cos \alpha \sin \theta - \left( \frac{z_T - z_w}{D} \right) \sin \alpha \right] \quad (69)$$

where  $\theta$  is the angle formed by the missile longitudinal axis and a line between the detonation point and the target centroid,  $(x_w, y_w, z_w)$  is the detonation point coordinate of the warhead  $\alpha$  and  $\theta$  are the warhead terminal flight path angles at time of detonation and  $D$  is the distance from the warhead to the target given by:

$$D = \left[ (x_w - x_T)^2 + (y_w - y_T)^2 + (z_w - z_T)^2 \right]^{1/2} \quad (70)$$

The resulting fragment striking elevation angle is given by:

$$\phi = \sin^{-1} \left[ (z_w - z_T) / D \right] \quad (71)$$

At this point, the distance to the target and the fragment classes which strike the target are known. To calculate the striking density of fragments of each class, the initial dynamic velocity ( $V_0$ ) must be calculated as follows:

$$V_0 = V_m \cos \phi + (V_{s_k}^2 - V_m^2 \sin^2 \phi)^{1/2} \quad (72)$$

where  $V_m$  is the missile terminal velocity,  $V_{s_k}$  is the static initial velocity for the fragments of the  $k^{th}$  class, and  $\phi$  is as computed in Equation (69). Finally, the dynamic fragment striking density,  $\rho_{D_k}$ , is computed by:

$$\rho_{D_k} = 2\rho_{s_k} V_0^3 / \left[ D^2 V_{s_k} (V_0^2 + V_{s_k}^2 - V_m^2) \right] \quad (73)$$

where  $\rho_{s_k}$  is the static fragment density (fragments per steradian) of the  $k^{th}$  class, and  $V_0$  is defined by Equation (72).

The remaining tasks are to solve by iteration for the striking velocity and to compute  $Av_k$  for  $k = 1, \dots, N_c$ , by interpolating in the tabular vulnerability data. Thus, the kill probability due to fragments ( $PK_F$ ), as defined by Equation (67) may now be calculated.

It should be reiterated at this point, that the concept of vulnerable area, although it is the best concept available, is certainly imperfect and may be considered approximate in simulating real life situations between highly accurate terminally guided munitions and actual three-dimensional targets. The most glaring inadequacy is that the vulnerable area concept is not three-dimensional or even truly two-dimensional in that the VA associated with a vulnerable component is all assumed to be located at a specific point (the component centroid). Hitting or missing a vulnerable component (of any size is mathematically assumed to depend on whether or not the component centroid is within the fragment spray zones. Even the most sophisticated of surface target computer programs utilize this imperfect concept although some allow for the VA to be partitioned among several point locations rather than a single one.

Most of the effort to develop better concepts is being directed toward improved air target effectiveness programs where the extent of the concept inadequacy and hence the need for improvement is greatest. However, one new concept for development of superior surface target

effectiveness methodology is the extension of the POINT BURST vulnerability assessment routines (e.g., Reference 52) to the calculation of endgame effectiveness of surface targets. This effort is currently being conducted at AFATL.

#### Multiple Fragment and Synergistic Effects

Fragmentation kill probability ( $P_{KF}$ ), as computed by the above methodology, is restricted to the precept that fragmentation damage is invariably the result of a single fragment penetration into a single vulnerable component. There is no allowance for the real-life possibility that one fragment might penetrate the shielding and a second (following) fragment could damage the vulnerable component behind the shield, or that the simultaneous impact of many fragments might cause damage in excess of that which would be caused by the same number of fragment hits, one at a time. Only recently has much thought been given to the possible bonus effects of multiple fragment or synergistic damage mechanisms. Recent developments in the focusing of kinetic energy fragments, primarily for antiaircraft weapons, has added an impetus to develop realistic methodology to account for these recognized phenomena. Thus far, most of the methodology has concentrated on redefining the vulnerability to include essential structural components which were previously considered only as shielding. The damage mechanisms are basically of two types, "Energy Density" or "Material Removal." For the former, a threshold energy density is defined and if the kinetic energy of all the fragments within a unit area collectively exceeds this value at the time of impact the target is sufficiently damaged. This concept assumes that all of the fragment kinetic energy is transferred to the target (the fragments do not penetrate). The second concept is almost the antithesis of the first in that it assumes complete penetration of each fragment, removing the structural material from each fragment hole and infers that the damage results from weakening the structure sufficiently so that normal static and dynamic loads cause complete failure. Although much attention has been devoted to these concepts, the resulting methodologies are not yet widely accepted and are seldom, if ever, used in evaluation of surface target weapon lethality.

## SECTION V

### MISCELLANEOUS SPECIAL PURPOSE VULNERABILITY METHODOLOGY

The previous sections on direct hit, blast, and fragmentation vulnerability were attempts to describe the methodology available in more than 90 percent of the endgame effectiveness analysis computer programs. There are perhaps three other conventional kill mechanisms worthy of a brief mention. These include incendiary/fragmentation weapons, shaped charge weapons, and flechette weapons. The following paragraphs present a very cursory discussion of the most significant methodologies which are unique to these particular kill mechanisms. There are also several continuous rod warhead types in the inventory, but these warheads are used exclusively for air targets and will not be included in this surface target report.

#### INCENDIARY/FRAGMENTATION MUNITION MODELS (REFERENCES 53 THROUGH 58)

The most inclusive treatise on effectiveness of incendiary or incendiary/fragmentation munitions examined is contained in the computer program documentation of Reference 56 and 57 which presents a description of a computerized spatial-time model of events potentially leading to ignition of fuel vapors by exposure to a mix of fragmentation and incendiary munitions or to munitions containing burning reactive metal particles. Thus, vehicular targets (e.g., trucks) containing fuel, become considerably more vulnerable when incendiary materials or reactive metal particles are added to the conventional fragmentation munitions.

The salient events occurring during an encounter between a reactive fragmentation munition and a target with flammable fuel are as follows:

- The munition or munitions detonate and project large primary fragments and numerous small burning particles of incendiary or reactive material.
- The primary fragment perforates the fuel container wall, passes through the fluid, and causes a cavity to expand in the fluid.

- The cavity begins to collapse half-way through its period and forces a highly atomized spray of fuel through the perforation during completion of its period.
- The fuel spray travels in a conical pattern away from the container wall as the cavity repeats successive pulses whose volume and duration are degraded until a steady leak results.
- The burning particles can interact with the fuel spray or with the resultant puddle of leaked fuel and cause ignition if the interaction occurs after spray emergence and prior to particle burnout.
- The ignition can propagate to the main fuel discharge and a sustaining fuel fire results.

Since gasoline is highly flammable at most ambient temperatures, a sustained fire is readily achieved due to the surplus of vapors in the local area. However, diesel fuel does not vaporize at most ambient temperatures and, although igniting the highly atomized fuel spray by burning particles is easily accomplished, a sustained fire is much more difficult to achieve. A considerably narrower lethal time span for sustained ignition of diesel fuel by burning particles exists than for Mogas. In particular, it appears that a significant delay in ignition time enhances probability of sustaining a fire to the main discharge stream since the spray is fully exposed, it delivers a larger thermal pulse, and the spray is not consumed prior to main stream issue.

#### Burning Particle Projection

Static particle projection characteristics are (as with normal fragments) defined in polar zones, each of which may have distinct values for:

- Upper and lower polar angles limiting distribution ( $\phi_u$  and  $\phi_l$ ).
- Number of particles ( $N_p$ ).
- Lethal burn time ( $t_b$ ).
- Initial velocity ( $V_0$ ).

- Drag coefficient limits ( $K_1$  and  $K_2$ ).

The burning particles are assumed to be launched in spherical segments formed by  $\phi_u$  and  $\phi_c$ . They obtain a constantly increasing radial distribution during flight due to uniform distribution of drag factors between  $K_1$  and  $K_2$ . Therefore, at any time from detonation, the burning particles are located in a solid spherical segment defined by the polar angles and outer and inner radii:

$$R_O(t) = 1/K_1 \ln(K_1 v_1 t + 1) \quad (74)$$

$$R_I(t) = 1/K_2 \ln(K_2 v_0 t + 1) \quad (75)$$

#### Fuel Container Perforation

The large primary fragments launched at munition detonation, impact and perforate the fuel container. The Project THOR equations (Reference 48) are used to determine perforation capability and residual mass and velocity of these fragments. The maximum azimuth deviation from the container surface normal is related to impact velocity ( $v$ ), mass ( $m$ ), elevation angle (ELEV), and wall thickness ( $T_e$ ) as follows:

$$AZ_{MAX} = AZ(v, m, T_e, ELEV) \quad (76)$$

The residual velocity ( $v_R$ ) and mass ( $m_R$ ) were also related to impact characteristics as follows:

$$v_R = v_R(v, m, \theta, T_e) \quad (\text{fps}) \quad (77)$$

$$m_R = m_R(v, m, \theta, T_e) \quad (\text{gr}) \quad (78)$$

---

\*The specific functions are not identified in this text to avoid security classification. For further detail see Reference 57.

where  $\theta$  is obliquity, given by:

$$\theta = \cos^{-1} [\cos (AZ) \cos (ELEV)] \quad (79)$$

The fragment is assumed to cause a perforation size equal to its presented area ( $A_p$ ).

#### Fuel Cavitation and Spray Emergence

After the primary fragment has perforated the fuel container wall, the residual fragment begins to pass through the fluid. A cavity is formed in the fuel behind the residual fragment. The volume and period of the cavity has been shown to vary with fragment kinetic energy as follows:

$$V_c = 8.92 \times 10^{-7} E \quad (\text{cc}) \quad (80)$$

$$\tau = 9.85 \times 10^{-6} \sqrt[3]{E} \quad (\text{sec}) \quad (81)$$

where  $E$  is fragment kinetic energy in ergs obtained from:

$$E = \frac{1}{2} m_R v_R^2 \quad (82)$$

Equations (80) and (81) were derived from underwater ballistic experiments.

Assuming the cavity achieves its maximum extension at one half of its period, then the fuel spray begins to emerge from the fragment perforation at time  $\tau/2$  seconds after impact when the cavity begins to collapse. Emergence velocity of the spray, assuming uniformity, is given by:

$$v_s = 0.30 V_c / [(\tau/2) (A_p)] \quad (83)$$



The spray emerges from the container in a conical pattern normal to the surface within a cone angle of approximately 20-degrees. The outer and inner diameter limits of the spray  $D_O$  and  $D_I$  are expressed as a function of time (t) from detonation as follows:

$$D_O(t) = \begin{cases} 0 & \text{if } t \leq t_f + \tau/2 \\ (1/K) \ln [Kv_s (t - t_f - \tau/2) + 1] & \text{otherwise} \end{cases} \quad (84)$$

$$D_I(t) = \begin{cases} 0 & \text{if } t \leq t_f + \tau \\ (1/K) \ln [Kv_s (t - t_f - \tau) + 1] & \text{otherwise} \end{cases} \quad (85)$$

where K is drag coefficient of the fuel droplets, and  $t_f$  is the primary fragment time of flight, given by:

$$t_f = (e^{K_f R} - 1) / (v_i K_f) \quad (86)$$

where  $K_f$  is drag coefficient for the primary fragment, R is distance from detonation point to the fuel container, and  $v_i$  is initial velocity of the primary fragment. Equations (84) and (85) define location of the first fuel spray in front of the container in terms of time from detonation.

It should be noted that wall thickness ( $T_e$ ) of the fuel container is the only target parameter in these equations. Fuel spray characteristics are sensitive to other target parameters including container size, container shape, ullage/fuel ratio, impact point relative to fuel head as well as fragment configuration and mechanical properties. These relations are based on full 5-gallon military fuel cans impacted at the center by steel fragments.

#### Fuel Cavitation and Spray Pulses

The initial fuel cavity collapses and begins to expand again with a somewhat degraded maximum volume and period. As many as five consecutive pulses of fuel spray have been observed during tests against full 5-gallon fuel cans. However, three pulses were observed in most

cases; thus, the model enables the program user to evaluate effects of up to three pulses.

The time from impact when the first fuel pulse issues from the container is given by:

$$t_1 = \tau_1/2 \quad (87)$$

where  $\tau_1$  is the period of the first pulse, given by Equation (81).

The empirical approach involved establishing a value for  $\alpha$  which forces the following equations to fit observed issue times for the second and third pulses:

$$t_2 = \tau_1 + \alpha \tau_1/2 \quad (88)$$

$$t_3 = \tau_1 + \alpha \tau_1 + \alpha^2 \tau_1/2 \quad (89)$$

This establishes a degradation factor for the period of each consecutive pulse. Additionally, the cavity volume at maximum extension was degraded as follows:

$$V_{c2} = V_{c1} / (1 + \alpha/2) \quad (90)$$

$$V_{c3} = V_{c1} / (1 + \alpha + \alpha^2/2) \quad (91)$$

where  $V_{c1}$  is maximum volume of the first cavity [Equation (80)], and  $V_{c2}$  and  $V_{c3}$  are volumes of the second and third cavities. A value for  $\alpha$  of 0.7 has been derived from high speed film of gun tests. This value provides good correlation with observed times of  $t_2$  and  $t_3$ , and also correlates well with spray issue velocity calculated by Equation (83). A space-time history of the second and third pulses is established by recycling through Equations (83), (84), and (85) using modified data for cavity volume and period.

If the primary projectile perforates the container beneath the fuel level but near a free surface, the cavitation phenomenon is not expected to behave with no edge effects as described above. However, the nature of events involved in the cavitation process are of such complexity as to preclude their formulation from a purely theoretical standpoint.

#### SHAPED CHARGE MUNITION MODELS

A second class of special purpose surface target programs consists of shaped charge simulation models for both conical and linear shaped charge munitions. The shaped charge munitions take advantage of the focusing properties exhibited by a detonation wave encountering a cavity or channel which is normal to and symmetric with the advancing detonation wave front. Figure 15 illustrates both a conical shaped charge and a linear shaped charge. The primary kill mechanism for both weapons is an ultra high-velocity jet of molten metal which is highly efficient in penetrating structural materials or armor.

A direct hit by a conical shaped charge munition will produce penetration of from 4 to 6 calibers through hardened armor plate. This means that a 6-inch-diameter munition will consistently penetrate from

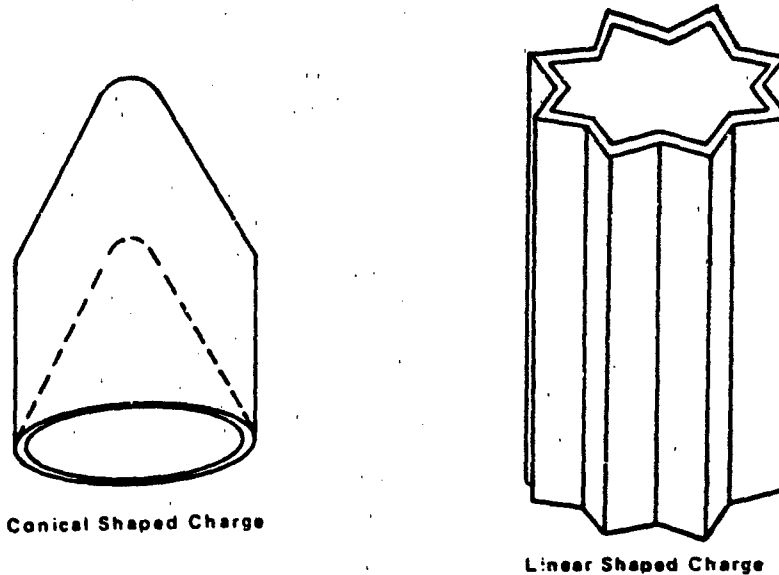


Figure 15. Shaped Charge Geometry

24 to 36 inches of armor. Most direct hit programs for conical shaped charge munitions assume a penetration probability of unity and merely compute the probability that a randomly located penetration shotline will impact a vulnerable component. Reference 59 is an example of a highly accurate conical shaped charge evaluation program.

Linear shaped charge evaluation methodology is more complicated since there are several separate kill mechanism sources, and each is a line source of high velocity, molten-metal jet rather than a point source. An example of a typical formulation for a linear shaped charge evaluation program follows (from Reference 60).

In defining linear shaped charge warheads for effectiveness computations, it is necessary to evaluate three kill mechanisms: blast, jet-slug, and fragmentation effects. Each kill mechanism is capable of inflicting kills on targets by severe structural damage. The target structure may be represented as previously discussed in Section II.

A linear shaped charge warhead will have blast kill potential equivalent to a slightly smaller conventional warhead except in the jet-slug zones, where the blast kill will be enhanced by increased overpressure and consequently higher blast kill capability. To model the shaped charge blast kill, the blast ellipsoids are defined and checked initially for conventional blast kill. If the target is not killed by conventional blast, a second set of larger blast ellipsoids is checked to determine if the target is within lethal range of the enhanced blast. The final check will be to determine if the blast center is contained within the warhead jet-slug zones. The probability that the target is killed by the damage mechanism is called  $P_B$ .

A linear shaped charge warhead also projects slugs or rods within the jet-slug zone oriented parallel to the warhead centerline. Up to three of these slugs for each jet may be projected. The slugs are described by mass, cross section, ballistic data, initial velocity and flyoff direction. The slugs are projected along the centerlines of the angular segments representing the jet-slug zone. Target vulnerability to slug impact is defined by a series of ellipsoids representing structural components. Encounter geometry, slug velocity, drag, and direction is used to establish the event of a slug-target intercept with the target ellipsoids. Each ellipsoid has a conditional kill probability assigned for slug impacts. The probabilities are combined statistically, assuming independent events, for more than one impact into the probability of kill due to jet-slug ( $P_J$ ).

In addition to slugs, fragments with a spectrum of masses, initial velocities, and drag characteristics are projected from each linear shaped charge liner. The capability for representing several classes of fragments is provided. The fragment spray is limited by two angles measured from the forward and aft ends of the warhead, and an angular increment about the warhead centerline.

Target vulnerability is represented by a vulnerable area centered about one or more points. If a vulnerable point is established to be in one of the fragment sprays, then kill probability due to fragments is computed by:

$$p = 1 - \text{EXP} \left( - \sum_{i=1}^N \rho_i AV_i \right) \quad (92)$$

where  $\rho_i$  is impacting fragment density of the  $i^{\text{th}}$  class,  $AV_i$  is target vulnerable area of the  $i^{\text{th}}$  class, and  $N$  is the number of fragment classes striking the target. The computer program formulation includes the capability to input tabular vulnerable area as a function of fragment mass, velocity, and striking aspect. The capability for computing structural kill from multi-fragment impact is also included.

The basic geometry for a specific weapon-target encounter, including aim point, guidance error, fuzing point, and detonation point, is established identically for linear shaped charge warheads as for conventional fragmentation munitions. However, techniques for computing fragmentation kill probability for conventional warheads, assuming a point source of fragments, are not adequate for evaluating linear shaped charge warheads because of the narrow polar beam spray zone (on the order of 5 degrees) which includes all fragments projected by the warhead. For example, the width of a 5 degree beam spray at a distance of 50 feet from the point warhead is < 5 feet, thus a warhead length of 1 foot would constitute an error of 20 percent in the actual beam spray width if a point source of fragments were assumed. The following paragraphs present techniques for correcting beam spray zone width to account for warhead length.

The fragmentation subroutine for the conventional warhead computer program starts to compute fragment kill with a target description and a warhead detonation point ( $X_D$ ,  $Y_D$ ,  $Z_D$ ). The point of fragment-target

intercept  $[X_s(i, j), Y_s(i, j), Z_s(i, j)]$  is found which determines the points where fragments projected from the warhead with velocity  $i$  hit the target vulnerable component  $j$ . For an intercept, the polar angle  $\theta_F$  from which the fragments of the warhead were projected to strike the target component is computed. This angle is then compared to the forward and aft beam spray angles  $\theta_1$  and  $\theta_2$  to determine if the solution is valid ( $\theta_1 < \theta_F < \theta_2$ ). For a linear shaped charge, the values of  $\theta_1$  and  $\theta_2$  must be modified to account for warhead length.

Figure 16a is a diagram of the current fragmentation model for a cylindrical warhead showing the warhead detonation point  $(X_D, Y_D, Z_D)$ , the point where the fragments strike the target vulnerable point  $(X_s, Y_s, Z_s)$ , the forward and aft polar angles  $\theta_1$  and  $\theta_2$ , and the angle to the target  $\theta_F$ . With this model it is obvious that the vulnerable point is outside the mathematically defined beam spray zone ( $\theta_F < \theta_1$ ) and the solution would be rejected. Figure 16b shows how the target vulnerable point can be included in the beam spray and establishes the geometry for formulating equations to correctly model the fragment-target intercept.

The formulation is as follows:

From Figure 16a the distance of fragment flight  $D_f$  is given by:

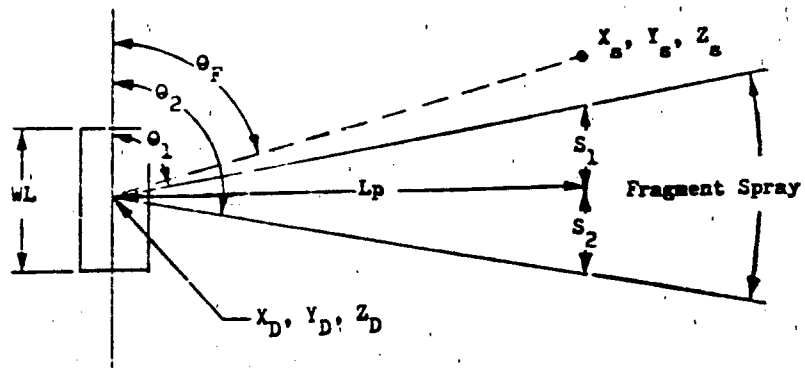
$$D_F = [(X_s - X_D)^2 + (Y_s - Y_D)^2 + (Z_s - Z_D)^2]^{1/2} \quad (93)$$

The perpendicular distance  $L_p$  from the warhead centerline to the target vulnerable point is given by:

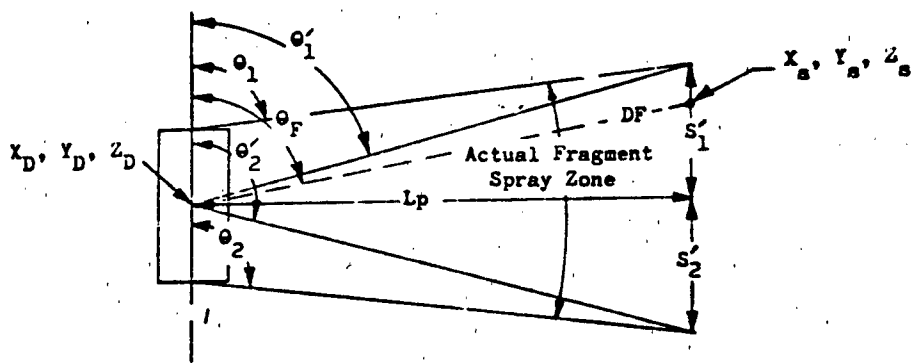
$$L_p = (D_F)(\sin \theta_F) \quad (94)$$

The width of the forward beam spray at the perpendicular distance  $L_p$  is defined in the point source model (Figure 16a) by:

$$S_1 = \frac{L_p}{\tan \theta_1} \quad (95)$$



(a) Point Source (Uncorrected)



(b) Line Source (Corrected)

Figure 16. Fragment Spray Representation

The width of the aft beam spray at the perpendicular distance  $L_p$  is defined by:

$$S_2 = - \frac{L_p}{\tan \theta_1} \quad (96)$$

Adding one-half the warhead length ( $W_L$ ) as shown in Figure 16b to each value gives:

$$S_1' = \frac{L_p}{\tan \theta_1} + \frac{W_L}{2} \quad (97)$$

$$S_2' = - \frac{L_p}{\tan \theta_2} - \frac{W_L}{2} \quad (98)$$

The corrected angles  $\theta_1'$  and  $\theta_2'$  are then given by:

$$\theta_1' = \tan^{-1} \frac{L_p}{S_1'} \quad (99)$$

$$\theta_2' = \tan^{-1} \frac{L_p}{S_2'} \quad (100)$$

If  $\theta_F$  is between the corrected values  $\theta_1'$  and  $\theta_2'$  ( $\theta_1' < \theta_F < \theta_2'$ ) the vulnerable point will be in the fragment beam spray.

The density of fragments which strike the target must also be established to compute kill probability. Hence, techniques employed for point-source fragmentation cannot be directly applied for evaluating a linear shaped charge warhead. The equation which determines the dynamic striking fragment density for conventional fragmentation warheads can be employed with two changes:



- Use the modified polar angles,  $\theta_1'$ , and  $\theta_2'$ , to account for warhead length.
- Multiply by a factor of  $2\pi/\Delta\gamma$ , where  $\Delta\gamma$  is the roll angular increment containing the fragments projected from a liner, to reflect the fact that a linear shaped charge warhead is not isotropic.

Kill probabilities due to fragmentation ( $P_f$ ) are determined accounting for fragment drag, impacting density, mass, velocity, angle, and dynamic missile velocity.

Thus, all three kill mechanisms for a linear shaped charge are accurately defined and the total kill probability ( $P$ ) resulting from blast, jet slugs, and fragmentation is then formulated as:

$$P = 1 - (1 - P_B) (1 - P_S) (1 - P_F) \quad (101)$$

#### FLECHETTE PROJECTING MUNITION MODELS (REFERENCES 60 and 61)

Warheads which project flechettes as a kill mechanism may be assumed to be special cases of fragmentation warheads. Flechettes may be thought of as stabilized, streamlined fragments which travel through the airstream like darts or arrows presenting little aerodynamic resistance and thus retaining their velocity over long distances.

The major differences in evaluating flechettes and fragments is in the distribution patterns and trajectory ballistics. Flechette patterns are severely limited in the maximum divergence angles, and because they maintain a lethal velocity for long distances, the effects of gravity cannot be neglected. The following paragraphs present an example of flechette methodology for personnel target lethal area computation from Reference 59. Similar program formulations are available for material and mixed (personnel-material) targets.

The warhead is assumed to release flechettes in a conical pattern with prescribed angular limits defined by a beam spray half angle measured off the longitudinal axis of the warhead. The flechettes can be distributed within this conical pattern in a uniform or normal manner, determined by an indicator in the input data. Beam spray half angles are

limited to 30 degrees or less and the warhead is assumed to be symmetric about a vertical plane containing the longitudinal axis. The conical pattern defined at release is subdivided into increments along the beam spray half angle, measured off the longitudinal axis of the warhead, and further divided into radial increments measured around and perpendicular to this axis (Figure 17). These angular increments of the flechette pattern are then projected into the ground plane by trajectory simulations. The program is capable of simulating a warhead containing up to three distinct classes of flechettes defined by:

- Flechette mass.
- Initial flechette velocity.
- Beam spray angle and angular increments.
- Distribution and number of flechettes.
- Flechette reference diameter.
- $C_D$  versus Mach number curve.

In addition, up to five sets of flechette reference diameters and/or  $C_D$  versus Mach number curves may be used as a function of real time

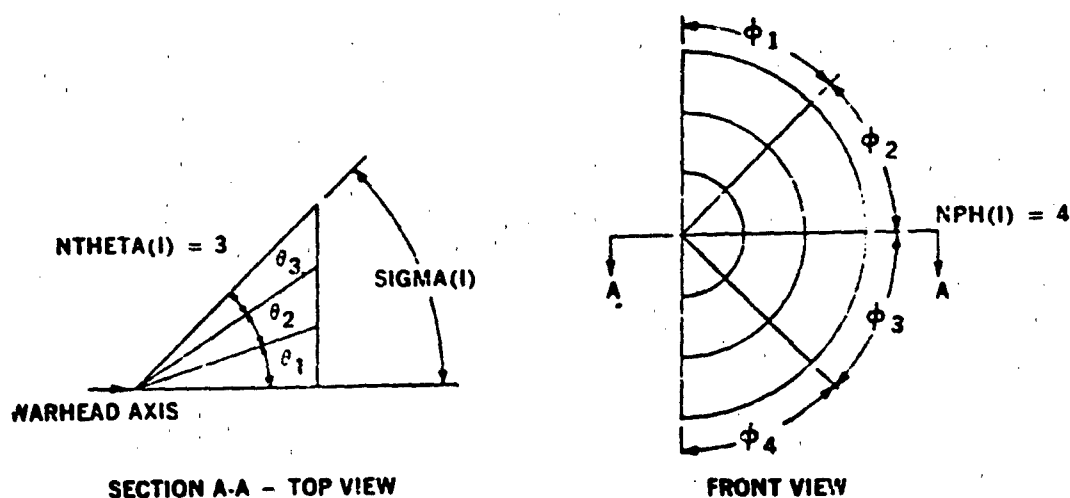


Figure 17. Sample Warhead Geometry

of flight for each class of flechettes. This capability enables the simulation of unstable flechette flight.

The Flechette Lethal Area Program was compiled to evaluate the lethal area of flechette projecting warheads against personnel targets. Munition lethal area is established by integrating kill probability against either standing or prone troops or troops crouching in foxholes within the impact pattern area. Vulnerability of personnel targets is defined in terms of target presented area and a conditional kill probability established for a hit on the target. Presented area of the target is a function of the orientation of the flechette at impact. Conditional kill probability is established through a casualty criterion equation which utilizes flechette mass, striking velocity, and three constants defining the kill criterion (see Reference 61).

Terminal delivery conditions of the missile are significant in that a damage assessment point in the lethal area grid must be determined by integrating the equations of motion from specified initial conditions. Velocity and direction of a given flechette at release predetermines the point of impact in the ground plane. The warhead, as discussed above, is subdivided into a grid defining orientation of a flechette dispersion pattern, where each point in this pattern is integrated through time to establish an impact pattern in the ground plane. Release geometry at launch is defined relative to the missile coordinate system.

Initial velocity ( $V_M$ ) imposed on flechettes is determined relative to the ground plane. This is the total velocity of the flechette and represents the vector sum of the missile velocity and any ejection velocity associated with the dispersion mechanism. At the time of release, stability of the flechette becomes a problem that is not readily defined. However, the tumbling of an unstable flechette may be simulated by adjusting a portion of the drag curve where instability would occur. Since the reference diameter is directly proportional to the drag it may also be altered to account for instability. Up to five sets of flechette diameters and/or  $C_D$  versus Mach number curves may be input for each class. These data are a function of time of flight and enable the simulation of tumbling, oscillating, and stable motion. A smaller time increment of integration may be employed in the trajectory computation for a specified period of time following a change from one set of drag data to another. This is to ensure accuracy in the iterative solution of the equations of motion.

Height of release is defined by input data and is common for all classes of flechettes. This program was especially designed to cope with

high altitude release, as the gravity effects are more influential for this terminal release condition.

The warhead terminal attack angle (measured positively downward from the horizontal to the nose of the missile) is input to relate the flechette flight direction to the ground. This is necessary as the dispersion pattern is defined relative to the missile axis, and some relationship must be established between its orientation and the impact plane. Gravitational forces are assumed to be normal to the ground plane.

The methodology contained in the Flechette Lethal Area Program was formulated from basic mathematical and physical equations. It may be subdivided into three orderly sections discussed in detail below.

#### Warhead Methodology

The simulation of a flechette dispersing warhead is formulated by geometrically establishing an ejection grid, relative to the warhead or missile axis as discussed above. Each point in this pattern is associated with the directional vector of a flechette at the time of release. The vector is assigned an initial velocity obtained from the input data and is transformed into its three components along the coordinate axes of the ground reference system. These three velocity components given by  $V_X$ ,  $V_Y$ ,  $V_Z$  are then used in solving the equations of motion for the trajectory routine.

#### Trajectory Analysis (Figure 18)

All effectiveness methodology currently available contains the assumption that fragments fly straight line trajectories from warhead to the target. This assumption is valid if velocity is high, distance to the target is low, and hence time of flight is small. However, flechettes launched at high altitudes have a relatively long flight time; thus, gravity significantly affects the trajectories of the flechettes. To accurately account for these effects the equations of motion must be integrated from specified initial conditions (velocity and direction) at launch, through time and space, to impact. The lethal area integration grid must be established by initial conditions of projectiles at the warhead point of detonation. The equations of motion defining the flight of each flechette are derived from Newton's second law where the drag force is given by:

$$F_D = 1/2 C_D \rho A V^2 = - M \frac{dv}{dt} \quad (102)$$

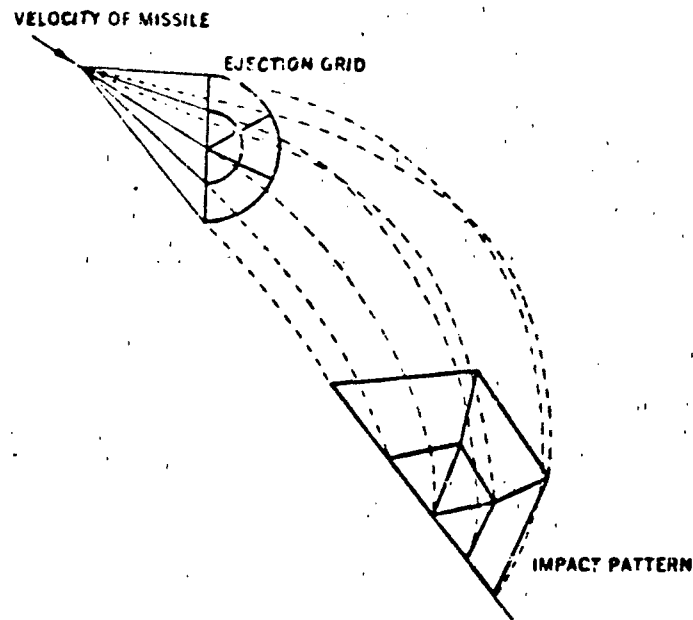


Figure 18. Trajectory Geometry

Expanding this formula into component forms relative to the ground reference system, the equations of motion for a given flechette can generally be described by:

$$\ddot{X} = - (1/2 C_D \rho A / M) (V)(V_x) \quad (103)$$

$$\ddot{Y} = - (1/2 C_D \rho A / M) (V)(V_y) \quad (104)$$

$$\ddot{Z} = - (1/2 C_D \rho A / M) (V)(V_z) - g \quad (105)$$

where  $C_D$  is the drag coefficient,  $\rho$  is the density of air,  $A$  is the presented area of the flechette,  $V_x$ ,  $V_y$ ,  $V_z$  are the velocity components of

the flechette velocity vector  $V$ ,  $M$  is the flechette mass, and  $g$  is the acceleration of gravity.

### Lethal Area Computations

Integration of Equations (103), (104), and (105) cannot be performed in closed form and requires a finite difference iterative procedure. The numerical solution of these equations is performed in the program by the method of Runge and Kutta. From the solution of these basic equations of motion, the striking velocity, impact angle, and the impact coordinates (relative to the point of release) of the flechettes in the ground plane can be determined. The impact pattern is determined by looping the above procedure for each point of release in the ejection grid. The polygons formed in the ground pattern by the impact coordinates are sequentially numbered as shown in Figure 19.

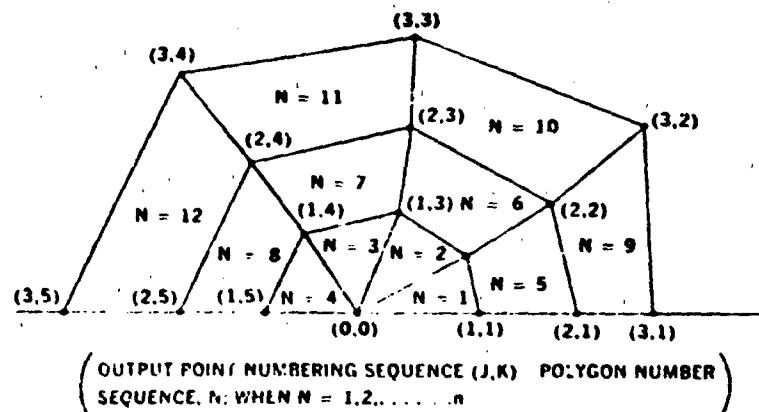


Figure 19. Sample Impact Pattern Geometry

As discussed above, methodology has been developed to evaluate munitions projecting up to three classes of flechettes. This makes it possible for the simulation to contain one, two, or three impact patterns which may or may not overlap each other. For the lethal area computations, the total impact pattern of all classes of flechettes is divided into two parts:

- Areas in the ground plane which contain flechettes from only one class.
- Areas in the ground plane which contain flechettes from two or more classes.

Lethal area computations are accomplished through a numerical integration of kill probabilities over all area. These kill probabilities can be easily calculated for areas in the ground pattern which contain flechettes from only one class; however, those areas in which the patterns overlap present a more complex solution. The program initially assumes that no overlap occurs, and the area of each polygon (N) in all class patterns is individually calculated. The impact angle and terminal velocity of flechettes at each polygon vertex is calculated in the trajectory portion of the program. An average or mean value of velocity and impact angle is calculated for each polygon using these data. In addition, density of the flechettes is calculated by taking the total number of flechettes in the original polygon (determined at release) and dividing by the polygon area at impact. Kill probability is calculated by:

$$PK(N) = 1 - e^{-\rho A_p P_C} \quad (106)$$

where  $\rho$  is flechette density in polygon N,  $A_p$  is presented area of the target,  $P_C$  is conditional kill probability. A preliminary munition lethal area is calculated by summing the product of kill probability and area for all polygons:

$$AL = \sum_{i=1}^K PK(N) (A(N)) \quad (107)$$

where K is the total number of polygons in all classes.

At this point in the program a check is made to determine if the ground patterns from the various groups overlap. If only one class of flechettes is being run, or if no overlap occurs, the munition lethal area is given by Equation (107). If two or more classes have flechettes falling in a common area, the overlap condition exists. Limits are then determined to localize the areas of overlap, and a rectangular grid of points is superimposed over this area. Each grid point is associated with

a prespecified area. The loss of lethal area (DALG) due to overlap is calculated for the incremental area associated with this grid point by:

$$DALG = AGRID \left[ \sum_{i=1}^J PK(i, N) - \left( 1 - \prod_{i=1}^J [1 - PK(i, N)] \right) \right] \quad (108)$$

where AGRID is grid incremental area,  $PK(i, N)$  is kill probability in polygon (N) of class (i), and J is the total number of polygons which contain the grid point.



## REFERENCES

1. Weapon Effectiveness, Selection and Requirements-Basic JMEM/AS (U), TH 61A1-1-1-1, Joint Technical Coordinating Group for Munitions Effectiveness, March 1972, Confidential.
2. Joint Munitions Effectiveness Manuals - Air-to-Surface (JMEM/AS) - Special Publications (U), TH 61A1-3 Joint Technical Coordinating Group for Munitions Effectiveness, No Date, Confidential.
3. Methodology Handbook (JMEM) (U), TH 61A1-3-6, Joint Technical Coordinating Group for Munitions Effectiveness, No Date, Confidential.
4. Technical Handbook Index, TH 61-1-2, Joint Technical Coordinating Group for Munitions Effectiveness, May 1971, Unclassified.
5. Einbinder, S. K., A Computer Program for Combining Weapon Damage Functions for Use in Matrix Computations, Technical Report 3530, AD 814 608L, Army Picatinny Arsenal, Dover, New Jersey, February 1967, Unclassified.
6. JMEM Computer Program for General Fuel Spray Personnel Mean Area of Effectiveness Computations, Volumes I and II (U), 61 JTCG/ME-70-6, Joint Technical Coordinating Group for Munitions Effectiveness, May 1971, Confidential.
7. Einbinder, S. K., Description of the Mathematical Model for Fraction Casualties and the Approximations Made in the Matrix Computer Programs, Information Report No. 16, Army Picatinny Arsenal, Dover, New Jersey, August 1968, Unclassified.
8. Distributed Aimpoint Program, AFATL Computer Program No. 2080, Undocumented Library Computer Program on Eglin Air Force Base Control Data Corporation 6600 Computer, Unclassified.
9. Einbinder, S. K., Expected Target Damage Computer Programs (Matrix Programs 100-1, 103, 105, and 106), Information Report No. 59, Army Picatinny Arsenal, Dover, New Jersey, February 1971, Unclassified.

10. Einbinder, S.K., Effectiveness Model for the Perforation of POL Drums, Technical Report 4291, Army Picatinny Arsenal, Dover, New Jersey, November 1971, Unclassified.
11. Snow, Roger, and Margaret Ryan, A Simplified Weapons Evaluation Model, Memorandum RM-5677-PR, AD 848 703, The Rand Corporation for United States Air Force Project RAND, Santa Monica, California, January 1969, Unclassified.
12. Taylor, William C., and Sidney Kravitz, A Method for Computing an Estimate of the Antipersonnel Effect of an Airburst Shell, Ballistic Research Laboratories Memorandum Report No. 555, AD 802 074, Army Ballistic Research Laboratories, Aberdeen Proving Ground, Maryland, August 1951, Unclassified.
13. Jarnagin, Milton P., Jr., Evaluation of Expected Casualty Area in Weapons Effectiveness Studies, NWL Technical Report TR-2113, AD 832 001, Naval Weapons Laboratory, Dahlgren, Virginia, February 1968, Unclassified.
14. Handbook of Air-to-Surface Weapons Analysis Programs, NOTS TP 4288, AD 824 043, Hughes Aircraft Company for Naval Ordnance Test Station, China Lake, California, June 1967, Unclassified.
15. Danish, Michael B., Single Shot Hit Probability and an Application to Vulnerability Analyses, BRL Memorandum Report No. 1875, AD 824 713, Army Ballistic Research Laboratories, Aberdeen Proving Ground, Maryland, October 1967, Unclassified.
16. Snow, Roger, Fast-Val: A Theoretical Approach to Some General Target Coverage Problems, Memorandum RM-4566-PR, The RAND Corporation for United States Air Force Project RAND, Santa Monica, California, March 1966, Unclassified.
17. Wang 700 Users' Manual for JMEM/AS Open-End Methods, Booz, Allen Applied Research for Joint Technical Coordinating Group for Munitions Effectiveness, April 1973, Unclassified.
18. Kline, Robert C., et al., Effect of Dependence Criterion on Hit Probabilities Associated with Multiple Warhead or Salvo Firings, NOLTR 66-37, AD 632 846, Naval Ordnance Laboratory, White Oak, Maryland, March 1966, Unclassified.

19. Dunn, Eldon L., A Handbook on the Effectiveness of Cluster Weapons Against Unitary Targets, NOTS TP 2383, AD 235 809, Naval Ordnance Test Station, China Lake, California, January 1960, Unclassified.
20. Garcia, M.A., A Markov-Process Approach in Estimating the Destruction of a Compound Target, TM-67-71, AD 823 967, Naval Missile Center, Point Magu, California, December 1967, Unclassified.
21. Garcia, M.A., A Method for Estimating the Lethality of an Anti-personnel Weapon Against a Compound Target, Technical Memorandum TM-68-11, AD 829 452, Naval Missile Center, Point Magu, California, February 1968, Unclassified.
22. Scherich, E. L., et al., Munition and Cluster Weapon Optimization Techniques, AFATL-TR-68-84, Martin Marietta Corporation for Air Force Armament Laboratory, Eglin Air Force Base, Florida, July 1968, Unclassified.
23. Ponder, Timothy C., and Frank A. Roescher, Major, USAF, Cylindrical Warhead Design Optimization, AFATL-TR-72-42, Air Force Armament Laboratory, Eglin Air Force Base, Florida, March 1972, Unclassified.
24. Airfield Attack Methodology, AFATL Computer Program No. 2093, Undocumented Library Program on Eglin Air Force Base Control Data Corporation 6600 Computer, Unclassified.
25. Nofrey, B.E., and J.R. Bok, Analysis of Straight-Path Penetration of Bodies Bounded by Quadric Surfaces, Technical Memorandum No. NMC-TM-64-41, Naval Missile Center, Point Magu, California, December 1964, Unclassified.
26. Bok, J.R., Analysis of Straight-Path Penetration of Multi-Layer Bodies of Rotation, Miscellaneous Publication No. NMC-MP-62-8, Naval Missile Center, Point Magu, California, October 1962, Unclassified.
27. Cudney, Donald E., and James B. Flint, Target Description Computer Programs, Techniques for Developing Input Data (U), NOTS TP 4238, AD 379 263L, Falcon Research and Development Company for Naval Ordnance Test Station, China Lake, California January 1967, Confidential.

28. Shot Generator Computer Program, Volumes I and II, 61 JTCG/ME-71-5, Joint Technical Coordinating Group for Munitions Effectiveness, July 1970, Unclassified.
29. Brooks, George W., and Harvey N. Lerman, Target Description and Vulnerability Program, AFATL-TR-72-129, Martin Marietta Corporation for Air Force Armament Laboratory, Eglin Air Force Base, Florida, June 1972, Unclassified.
30. Magic Computer Simulation, Volume I. User Manual, 61 JTCG/ME-71-7-1, Joint Coordinating Group for Munitions Effectiveness, July 1970, Unclassified.
31. Magic Computer Simulation, Volumes I and II. Analysts Manual Part I and II, 61 JTCG/ME-71-7-2, Joint Technical Coordinating Group for Munitions Effectiveness, May 1971, Unclassified.
32. Blomquist, M., Act V: A Second Generation Minefield Evaluation Computer Model, AFATL-TR-73-184, Biocentrics, Inc. for Air Force Armament Laboratory, Eglin Air Force Base, Florida, September 1973, Unclassified.
33. Cudney, Donald E., and David O. Fraser, Minefield Simulation (MINSIM I), Volume II. Analyst Manual, AFATL-TR-71-128, Booz, Allen Applied Research, Inc. for Air Force Armament Laboratory, Eglin Air Force Base, Florida, December 1971, Unclassified.
34. Cudney, Donald E., and David O. Fraser, Minefield Simulation (MINSIM II) Computer Model, Volume II. Analyst Manual, AFATL-TR-72-195, Booz, Allen Applied Research, Inc. for Air Force Armament Laboratory, Eglin Air Force Base, Florida, October 1972, Unclassified.
35. Fraser, David O., Minefield Simulation (MINSIM III) Computer Model, Volume II. Analyst Manual, AFATL-TR-73-183, Booz, Allen Applied Research, Inc. for Air Force Armament Laboratory, Eglin Air Force Base, Florida, August 1973, Unclassified.
36. Heaps, Wilson E., and Wilbur L. Warfield, Minefield Effectiveness Models and Computer Programs for Personnel, Vehicular, and Tank Targets, AMSAA Technical Memorandum No. 109, AD 887 401, Army Materiel and Systems Analysis Agency, Aberdeen Proving Ground, Maryland, June 1971, Unclassified.

37. Haberman, J.R., Predication of Target Casualties from Minefield Penetration Using Markov Processes, NWC TP 5121, Naval Weapons Center, China Lake, California, May 1971, Unclassified.
38. Messinger, Dr. Martin, A Mathematical Model for Anti-Personnel Minefield Analysis, Information Report No. 14, Army Picatinny Arsenal, Dover, New Jersey, September 1972, Unclassified.
39. Messinger, Dr. Martin, A Mixed Anti-Materiel, Anti-Personnel Minefield Model, Information Report No. 20, Army Picatinny Arsenal, Dover, New Jersey, November 1972, Unclassified.
40. Haberman, J.R., Minefield Effectiveness Using A Markov Process Technical Note 4073-25, Naval Weapons Center, China Lake, California, July 1970, Unclassified.
41. Blomquist, M., A Computer Based Minefield Evaluation System, Report No. 715, Biocentric, Inc., St. Paul, Minnesota, December 1971, Unclassified.
42. Computer Program Documentation, Roadcutter (JMEM), JTCG/ME-70-1, Joint Technical Coordinating Group for Munitions Effectiveness, No Date, Unclassified.
43. Computer Program Documentation, Cumulative Damage Program for Hangars (JMEM), 61 JTCG/ME-70-2, Joint Technical Coordinating Group for Munitions Effectiveness, No Date, Unclassified.
44. Computer Program Documentation, Runway Cutter (JMEM), 61 JTCG/ME-70-4, Joint Technical Coordinating Group for Munitions Effectiveness, No Date, Unclassified.
45. Jackett, E.C., A Computer Program for Simulating Penetration of Bomb Shapes Into Certain Soils to Determine the Resulting Crater Diameters and Depths, 61 JTCG/ME-71-1, Joint Technical Coordinating Group for Munitions Effectiveness, March 1971, Unclassified.
46. Nolden, Kathren L., Computer Program for Determining Vulnerability of Aircraft Shelters, Pillboxes, and Bunkers to Shaped Charges, KE Penetrators, and GP Bombs, AFATL-TR-73-104, Booz, Allen Applied Research for Air Force Armament Laboratory, Eglin Air Force Base, Florida, April 1973, Unclassified.

47. VAREA Computer Program, Volumes I and II, 61 JTCG/ME-71-6, Joint Technical Coordinating Group for Munitions Effectiveness, July 1970, Unclassified.
48. The Resistance of Various Metallic Materials to Perforation by Steel Fragments; Empirical Relationships for Fragment Residual Velocity and Residual Weight, Project THOR Technical Report No. 47, John Hopkins University for Army Ballistic Research Laboratories, Aberdeen Proving Ground, Maryland, April 1961, Unclassified.
49. Analytical Solutions for Fuze Functioning After Impacting in Branches and Tall Tropical Grass (DEP 14) (U), 61 JTCG/ME-72-6, Joint Technical Coordinating Group for Munitions Effectiveness, May 1973, Confidential.
50. Fuze Height of Burst Distribution in Grasses (DEP 18) (U), 61 JTCG/ME-73-10, Joint Technical Coordinating Group for Munitions Effectiveness, March 1973, Confidential.
51. Sperraza, Dr. J., Casualty Criterion for Wounding Soldiers, BRL TN 1486, Ballistics Research Laboratories, Aberdeen Proving Ground, Maryland, June 1962, Confidential.
52. Cudney, Donald E., and James B. Flint, Target Description Studies: Point Burst Computer Program (U), NOTS TP 4241, AD 381 543L, Falcon Research and Development Company for Naval Ordnance Test Station, China Lake, California, April 1967, Confidential.
53. Smith, Warren K., Ignition Chart for Firebomb Range Calorimeter Plates, Technical Note 40604-10, Naval Weapons Center, China Lake, California, December 1968, Unclassified.
54. Flame Report-A Revised Procedure for Evaluating Firebomb Effectiveness and Correlating Data (U), 61 JTCG/ME-72-12, Joint Technical Coordinating Group for Munitions Effectiveness, December 1972, Confidential.
55. Keller, James A., et al., Vulnerability of Foreign Cargo Vehicles to Mk 77 Firebombs (U), NWC TP 5351, Falcon Research and Development Company for Naval Weapons Center, China Lake, California, May 1972, Confidential.

56. Ingram, R.R., Jr., et al, Human Incapacitation Produced by Burns II Provisional Method for Predicting Incapacitation with an Application to Two Military Stress Situations (U), EATR 4298 Army Edgewood Arsenal, Maryland, September 1968, Confidential.
57. Kitchin, Thurman D., and John J. Flowers, Incendiary/Fragmentation Munitions Computer Program, AFATL-TR-73-18, Methonics Incorporated for Air Force Armament Laboratory, Eglin Air Force Base, Florida, January 1972, Unclassified.
58. Kitchin, Thurman D., and John J. Flowers, Incendiary/Fragmentation Munitions Systems Analysis (U), Volumes I and II, AFATL-TR-71-86, Methonics Incorporated for Air Force Armament Laboratory, Eglin Air Force Base, Florida, July 1971, Confidential.
59. Breitenstein, E. P., Conical Shaped Charge Effectiveness Program (U), NOTS TN 4034-41, Naval Ordnance Test Station, China Lake, California, No Date, Confidential.
60. Day, William R., et al, Weapon Optimization Techniques, AFATL-TR-71-170, Martin Marietta Corporation for Air Force Armament Laboratory, Eglin Air Force Base, Florida, December 1971, Unclassified.
61. Fouse, Alan G., An Evaluation of the Zero Antiaircraft Potential (ZAP) Weapon Effectiveness, NWL TP 5081, Naval Weapons Laboratory, China Lake, California, December 1970, Unclassified.

# INITIAL DISTRIBUTION

Hq USAF/SA	1
Hq USAF/XO	1
Hq AFSC/DOSR	1
AFFDL/PTS	1
ASD/ENYS	1
AUL (AUL-LSE-70-239)	1
AFLC/Tech Library	1
TAC/Tech Library	1
AFIT/Tech Library	1
Aberdeen Pg Gd/Tech Lib Div	1
AMXS-D/Aberdeen Pg Gd	1
NWL/Code GAV	1
DIA/DI-7E	1
NADC/SAED/SDE	1
NAVORD/NORD-552B	1
DDC	2
NWL/Tech Library	1
NWC/Code 40701	1
NWC/Code 4563	1
NWC/Code 4565	1
BRL/AMXBR-VL	1
Picatinny Ars/SMUPA-AD-C-S	1
Picatinny Ars/SMUPA-DW6	1
Hq AFSC/SDW	1
CINCUSAFE/INT	1
Hq USAF/RDQRT	1
US.S Army Waterways Exp Sta	1
MERDC/SMEFG-B5	1
NOL/NO (Code 433)	1
Chief Naval Material Comd	
Navy Dept/MAT 031B	1
Hq Marine Corps/AAW1	1
NSRDC/Code 1702	1
NSRDC/Code 1749	1
NSRDC/Code 174.1	1
Hq USAF/SAMI	1
Hq 4950 TESTW/TZHM	1
Ogden ALC/MMNOP	2
TANC/TRADOCLO	1
AFATL/DL	1
AFATL/DLOSL	2
AFATL/DLYV	4
AFATL/DLQ	1
AFATL/DLY	1



END

DATE  
FILMED

8-74